12-2010

Modulation of Alpha-Subunit VISIT-DG Sequence Residues Ser-347, Gly-351 and Thr-349 in the Catalytic Sites of *Escherichia coli* ATP Synthase.

Laura Elaine Brudecki
East Tennessee State University

Modulation of Alpha-Subunit VISIT-DG Sequence Residues Ser-347, Gly-351 and Thr-349 in the Catalytic Sites of *Escherichia coli* ATP Synthase

---

A thesis

presented to

the faculty of the Department of Biological Sciences

East Tennessee State University

in partial fulfillment

of the requirements for the degree

Master of Science in Biology

---

by

Laura E. Brudecki

December 2010

Dr. Michael Zavada, Chair

Dr. Cecilia McIntosh

Dr. Ranjan Chakraborty

Dr. Darrell Moore

Keywords: ATP synthase, *Escherichia coli*, VISIT-DG, Phosphate binding

ABSTRACT

Modulation of Alpha-Subunit VISIT-DG Sequence Residues Ser-347, Gly-351 and Thr-349 in the Catalytic Sites of *Escherichia coli* ATP Synthase

by

Laura E. Brudecki

Binding of inorganic phosphate (P_i) in ATP synthase catalytic sites is a crucial step for the synthesis of adenosine-5'-triphosphate (ATP). ATP is the fundamental means of cellular energy in almost every organism, and in order to gain insight into the regulation of ATP catalysis, critical amino acid residues responsible for binding P_i must be identified. Here, we investigate the role of highly conserved α-subunit VISIT-DG sequence residues αSer-347, αGly-351, and αThr-349 in P_i binding. Mutations αS347A/Q, αG351Q, αT349A/D/R, βR182A, and αT349R/βR182A were generated *via* site directed mutagenesis. Results from biochemical assays showed that αSer-347 is required for transition state stabilization and P_i binding whereas αGly-351 is only indirectly involved in P_i binding and most likely maintains structural integrity of the catalytic site. Results from preliminary experiments on αThr-349 mutants suggest that the residue may be involved in P_i binding; however, further investigation is required to fully test this hypothesis.

DEDICATION

To my late grandfather, Edward John Brudecki

ACKNOWLEDGEMENTS

My utmost appreciation goes out to Dr. Cecilia McIntosh and Dr. Ranjan Chakraborty for their tireless assistance on this manuscript.

I would also like to thank Dr. Moore and Dr. Zavada for their comments on the manuscript as well as their guidance in areas other than science.

Finally, without my friends and family I would not be where I am today. Thanks everyone.

CONTENTS

LIST OF TABLES

LIST OF FIGURES

CHAPTER 1

INTRODUCTION

Background

ATP synthase is an enzyme found in nearly every organism ranging from bacteria to humans. ATP synthase functions like a motor in order to generate the majority of cellular energy through the synthesis of adenosine-5'-triphosphate (ATP) from adenosine-5'-diphosphate (ADP) and inorganic phosphate (P_i).

ATP synthase possibly could be one of the most ancient enzymes present on Earth today. Homology between ATP synthase α and β proteins suggests that the gene duplication that gave rise to these two proteins occurred before the emergence of mitochondria (Cloud *et al.*, 1969; Walker, 1982).

In order for life to exist as we know it today, the formation of a barrier to the external environment, a cytoplasmic membrane, would have had to evolve. There are many hypotheses as to how this happened, but as Mulkidjanian *et al.* (2009) state, the paradoxical chicken and egg scenario arises when trying to set forth an explanation. A lipid bilayer could not exist without transport proteins or the cell would be excluded from the external environment altogether (Mulkidjanian *et al.,* 2009). On the other hand, membrane proteins, due to their insoluble nature, would not have existed without the lipid bilayer encompassing them (Mulkidjanian *et al.,* 2009). So which came first? Mulkidjanian *et al.* (2009) and references therein propose that the first forms of life could recruit abiogenically formed amphiphilic molecules to form envelopes similar to modern viruses, but there are other hypotheses as to the beginnings of life. Lane *et al.* (2010) propose a solution in the form of an abiotic lipid membrane.

Lane *et al.* (2010) discuss the origins of life at hydrothermal vents in the ocean. The type of vent discovered at the turn of the century, alkaline vents, have an inorganic membrane that creates a naturally occurring proton gradient (Lane *et al.*, 2010). In contrast to other hydrothermal vents such as black smokers, alkaline vents have a temperature around 70°C and a pH close to 10 (Lane *et al.*, 2010; Wade *et al.*, 2010). Lane *et al*. (2010) propose that these alkaline vents could have sustained early life and provided the necessary conditions for RNA replication. Moreover, the naturally occurring inorganic membrane would have necessitated the emergence of a cytoplasmic membrane in order for life to escape the vent world (Lane *et al.*, 2010). A layer of primordial lipids, hydrothermally synthesized hydrophobic substances, could have been formed along the chambers created by the vents, just underneath the inorganic crust of the Earth (Lane *et al*., 2010). Early life could have, at first, used this membrane before enzymatic lipid synthesis was possible (Lane *et al.*, 2010). Concomitantly, Mulkidjanian *et al.* (2008) take the stance that RNA and proteins preceded membranous cells, yet others (Segré *et al.*, 2001) propose that life originated in a lipid world or even a protein-less RNA-lipid world (Deamer, 2008; Poole *et al.*, 1998; Szostak *et al.*, 2001; Vlassov, 2005).

In order to move out of the inorganic membrane and synthesize lipids and other proteins, early life would need some way to generate energy. Some theorize that the first organisms generated energy *via* fermentation pathways (De Duve, 2002; De Duve, 2005). Lane *et al.* (2010) make clear that fermentation, the pathway which Haldane (1929) and De Duve (2005) say must have been used by early life forms, does not seem to be a property our Last Universal Common Ancestor (LUCA) would possess. Lane *et al.*

(2010) argue that most life today uses oxidative phosphorylation pathways, and those that do use fermentation pathways for ATP synthesis retain machinery needed for oxidative phosphorylation, such as proton-motive ATPases (Lane *et al.*, 2010). Fermentation does not require membrane bioenergetics; but active transport across the plasma membrane does and is necessary for homeostasis, uptake of nutrients, and flagellar motility (Lane *et al.*, 2010).

Above and beyond all of the previous points made by Lane *et al.* (2010) on why fermentation was not likely to be used by LUCA, he points out that bacteria and archaea have significantly different gene sequences for enzymes used in fermentation. Noting that bacteria and archaea both have similar ATP synthase enzymes, it would hold that there was a common ancestor possessing an ATPase of some sort (Lane *et al.*, 2010 and references therein).

The common ancestor between archaea and bacteria would have been nothing like any life forms we see on Earth today. Archaea and bacteria are different in so many ways: the glycerol moieties of the membrane phospholipids in all archaea and bacteria are of the opposite chiralities; with a few exceptions, the hydrophobic chains also differ, being based on fatty acids in bacteria and on isoprenoids in archaea; and in bacterial lipids the hydrophobic tails are usually linked to the glycerol moiety by ester bonds, whereas archaeal lipids contain ether bonds (Mulkidjanian *et al.,* 2009).

The presence of ATPases in almost every organism confirms an early development, but beyond that the use of the proton motive force itself is widespread. Peter Mitchell lists different organisms that take advantage of proticity and the ways in which they do so in his Nobel Lecture (Mitchell, 1978). For example, there is the proton

motive bacteriorhodopsin system of *Halobacterium halobium*, the proton motive pyrophosphatase of photosynthetic bacteria, and protic heating in fat cell mitochondria of hibernating animals. The rotatory flagellar motor of bacteria is driven by proticity. Moreover, there are proton motive ATPase and proton-coupled transporter systems in chloroplast envelope membranes, in the plasma membranes of moulds, yeasts, and higher plants, and also in the membranes of chromaffin granules and synaptosomes (Mitchell, 1978).

In bacteria and eukaryotic mitochondria and chloroplasts there are F-type ATPases which function in respiration to form energy (Mulkidjanian *et al.,* 2009). There are also V-type ATPases which are found in membranes of eukaryote vacuoles that serve as pumps (Mulkidjanian *et al.,* 2009). Mulkidjanian *et al.* (2007) propose that different types of ATP synthase may have arose from a RNA helicase and a membrane channel which came together and then integrated a translocated protein into the complex which then became a new subunit. This is the rationale by which Mulkidjanian *et al.* (2007) explain homologous and non-homologous subunits between the two types of enzymes.

Among the prokaryotic F-type and V-type ATPases there are both proton-translocating and Na^+-translocating forms (Mulkidjanian *et al.*, 2009 and refernces therein). The sodium ion binding sites within the F/V-ATPases are arranged nearly identical to one another (Mulkidjanian *et al.*, 2008). This infers that the common ancestor to these two types of ATPases could have been a sodium translocating enzyme (Mulkidjanian *et al.*, 2008). Differentiation of the two types could have stemmed from the organism in which the ATPase was incorporated.

When discussing the origin of eukaryotic cells, many people recall the theory of

an endosymbiotic relationship between two organisms where one ends up being engulfed and incorporated into the other cell. This is a good explanation of why mitochondria have a different genome. Martin and Muller (1998) describe an alternate basis for which this event took place in their 'Hydrogen Hypothesis.' According to their hypothesis, eukaryotes arose through a symbiotic association of an anaerobic, strictly hydrogen-dependent, strictly autotrophic archaebacterium (the host) with a eubacterium (the symbiont) that was able to respire but generated molecular hydrogen as a waste product of anaerobic heterotrophic metabolism (Martin and Muller, 1998).

As a result of this fusion, sodium ion transport as a mechanism for ATP synthesis may have become less imperative which may be why the use of Na^+-translocating ATPases is not as prevalent in eukaryotes. Perhaps some environmental selection pressure resulted in the development of strictly hydrogen transporters in which case there may have been a scenario in which a symbiotic relationship favored survival. However, many organisms that are pathogenic to humans still use the sodium motive force for ATP synthesis (Häse *et al.,* 2001).

History of ATP Synthase Research

In 1929 Karl Lohmann isolated adenosine-5'-triphosphate (ATP) from muscle and liver extracts (Langen and Hucho, 2008). In 1937 Kalckar uncovered a link between cellular respiration and ATP, and two years later Belitser and Tsibakova coined the term 'oxidative phosphorylation' (Feniouk, 2010).

In oxidative phosphorylation, ATP is generated when oxygen is reduced to water with electrons donated from NADH and $FADH_2$ (Nelson and Cox, 2005). The high energy electrons are transferred exergonically by a series of membrane-bound electron

carriers, and the free energy which is generated is coupled to the transfer of protons across an impermeable membrane to an area of higher concentration (Nelson and Cox, 2005). This generates an electro-chemical potential. Protons flow across the membrane down the concentration gradient through ATP synthase, a membrane protein that couples proton flow to phosphorylation of ADP (Nelson and Cox, 2005).

Many scientists proposed chemical intermediates by which oxidative phosphorylation could occur, and it was not until 1961 that Peter Mitchell proposed the chemiosmotic hypothesis in which he suggested that there were no chemical intermediates, rather there were membrane proteins that maintained a proton gradient generated by respiration and ultimately used by ATP synthase as described above (Feniouk, 2010; Mitchell, 1961). As with any scientific discovery, there are some discrepancies as to who actually made the discovery and who received credit for it. Prebble (1996) writes that Davies and Krebs published the essential elements of the chemiosmotic hypothesis nine years earlier but did not approach the concept with an actual hypothesis; hence, no actual experiments resulted from their statements (Prebble, 1996). Prebble (1996) closes his discussion stating that in this particular instance factors of advocacy, timeliness, potential for experimentation, and presentation were more important than primacy. Mitchell formalized the hypothesis, which, after much scrutiny, became the chemiosmotic theory, and in 1978 he was awarded the Nobel Prize in chemistry for his contribution to bioenergetics (Feniouk, 2010; Mitchell, 1978; Nelson and Cox, 2005).

In 1960 Efraim Racker and his lab purified a soluble ATPase and found that phosphorylation activity accompanied the enzyme (Penefsky *et al.*, 1960; Pullman *et al.*,

1960). The enzyme responsible for oxidative phosphorylation was termed Factor 1 or F_1. Due to its soluble nature, F_1 may be gently stripped from the membrane during purification while remaining functionally intact.

In 1977 Paul D. Boyer's group proposed the binding change mechanism by which F_1F_O ATP synthase functions (Boyer, 1979; Boyer, 2002). This mechanism is described below in the Function section. John E. Walker's lab is responsible for determining the genes that encode ATP synthase in the early 1980s, and in 1994 his group resolved the first x-ray crystallographic structure of F_1 (Abrahams *et al.*, 1994). Walker, Boyer, and Skou received the 1997 Nobel Prize in Chemistry for their work on the mechanism for the synthesis of ATP and the discovery of an ion-transporting enzyme (Feniouk, 2010; http://nobelprize.org/nobel_prizes/chemistry/laureates/1997/). Walker has continued to solve crystallographic structures of ATP synthase and has many structures under his name in the Research Collaboratory for Structural Bioinformatics (RCSB) Protein Data Bank online (Berman, *et al.*, 2000).

In 1997 Kinosita's lab performed single particle experiments that visually displayed the rotational catalysis of ATP synthase which will be discussed further in the Function section (Nakamoto *et al.*, 2008; Noji *et al.,* 1997). In 2004 Itoh *et al.* showed that ATP synthase could be mechanically driven using the γ-subunit as a handle for magnetic bead attachment. This work established the premise that understanding the manipulation of ATP synthase may be useful in developing nanomachines.

In order for ATP synthase to serve as a base model for the development of nanomotors, we must first understand the mechanism of the enzyme. Our lab has focused on understanding the role of key phosphate-binding amino acids within the α/β catalytic

sites of ATP synthase. We have identified five residues required for phosphate binding: αSer-347, βArg-182, αArg-376, βLys-155, and βArg-246. This thesis focuses on the work for αSer347, αGly351, and αThr349.

αSer347, αGly351, and αThr349 are part of the VISIT-DG amino acid residue sequence which has been highly conserved throughout evolution (Li *et al.*, 2009). More importantly, this residue sequence lies in close proximity to the phosphate binding subdomain of the catalytic site (Li *et al.*, 2009). Therefore, we hypothesized that the residues of the VISIT-DG sequence may be playing some important catalytic and/or structural roles within the catalytic sites. Selection of these three residues is discussed in more detail under the Modulation section.

Structure

The structure of ATP synthase is similar in all organisms with some residue sequences being highly conserved throughout evolution (Li *et al.,* 2009). The number of subunits varies across organisms, but the structure of each subunit is conserved. Eubacterial ATP synthase contains at least 22 subunits and eight different polypeptides (Nakamoto *et al.*, 2008). Thirteen of those subunits are membrane-bound (Nakamoto *et al.*, 2008).

E. coli ATP synthase consists of eight subunits that are divided into two sectors. The ~380kD, water-soluble F_1 sector contains subunits α_3, β_3, δ, ε, and γ, and is responsible for catalytic activity. The membrane bound F_O sector houses a, b_2, and c_{10} subunits and is the proton translocating sector (Boyer, 1997; Devenish *et al.*, 2000; Hong and Pedersen, 2008; Karrasch and Walker, 1999; Li *et al.,* 2009; Nakamoto *et al.*, 2008; Senior, 1988; Senior *et al.,* 2002). Figure 1.1 shows the arrangement of subunits as

described above. The membrane bound sector is designated 'F_O' for its sensitivity to oligomycin which is conferred by the oligomycin sensitivity conferring protein (OSCP) (Hong and Pedersen, 2008).

As mentioned previously, F_1 can be easily dissociated from F_O in a reversible fashion. However, dissociation renders F_1 an ATPase alone and F_O a passive proton pore (Nakamoto *et al.*, 2008). When F_1 is purified and gently removed from the water insoluble F_O sector, a proton gradient cannot be established (Nelson and Cox, 2005). Protons leak from the F_O pore just as fast as they are pumped by the electron transport chain (Nelson and Cox, 2005). When F_1 is returned to solution, it associates with F_O, plugs the leaky pore and coupling of electron transfer and ATP synthesis is restored. (Feniouk, 2010; Kresge *et al.*, 2006; Nelson and Cox, 2005).

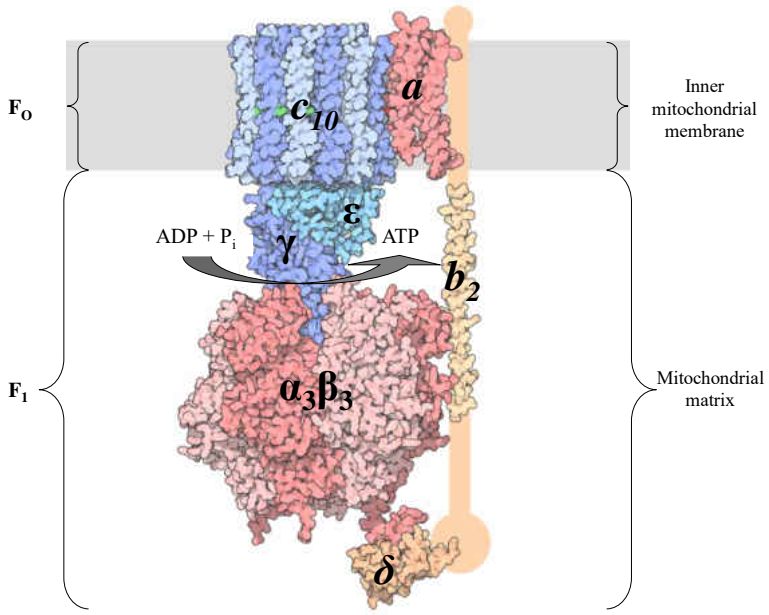

FIGURE 1.1 **Crystal structure of F_1F_O ATP synthase.** F_1 is from Bovine, and F_O and the stator are from *E. coli*. The image has been altered from the RCSB PDB Molecule of the Month by Goodsell (2005).

The $\alpha_3\beta_3$ oligomer is arranged like segments of an orange, alternating between α

and β. The α and β subunits are highly conserved. Seventy percent of the amino acids in bovine and *E. coli* ATP synthase are identical, and α and β proteins show persistent homology (Walker, 1982). The γ subunit consists of a coiled coil that goes up into the $\alpha_3\beta_3$ hexamer from its origin within the ring of *c* subunits as shown in Figure 1.1. Together, the γ, ε, and *c* subunits are the 'rotor' unit of the complex which is responsible for rotational catalysis (Nakamoto *et al.*, 2008). The 'stator' consists of the $\alpha_3\beta_3$ hexamer and subunit *a* (Nakamoto *et al.*, 2008). The pseudo hexamer is connected to *a* by the 'peripheral stalk' which is made up of two *b* subunits and one δ (Nakamoto *et al.*, 2008).

The number of *c* subunits is not known for every organism and the number is thought to vary among species. However, there is some structural information for subunit *c*. The membrane-embedded hydrophobic subunit consists of a hairpin of two helical trans-membrane segments connected by a short hydrophilic loop facing the F_1 sector (Nakamoto *et al.*, 2008). There is an essential carboxylic acid near the middle of the carboxyl terminal trans-membrane helix which is typically a glutamate, but in some bacteria the carboxylic acid is an aspartate (Nakamoto *et al.*, 2008). The number of *c* subunits varies between 10 and 15 depending on the species (Nakamoto *et al.*, 2008).

Little is known about subunits *a, b,* or δ mostly because there is no high resolution crystal structure of the subunits or of the interactions between the two *b* subunits and δ (Nakamoto *et al.*, 2008). With regard to subunit *a*, there are likely five transmembrane segments which interact with the ring of *c* subunits to assist in the translocation of protons (Nakamoto *et al.*, 2008).

Function

ATP synthase uses the proton motive force, and in some cases the sodium motive force, to drive ATP synthesis during oxidative and photophosphorylation (Nakamoto *et al.*, 2008). Oxidative phosphorylation occurs within the mitochondria of eukaryotes and the cytoplasmic membrane of bacteria (Bald *et al.,* 1998; Boyer, 1997; Weber and Senior, 1997) and archaea. Photophosphorylation occurs within the thylakoid membrane of chloroplasts (Bald *et al.,* 1998; Boyer, 1997; Weber and Senior, 1997) and cyanobacteria.

In oxidative phosphorylation ATP is generated when oxygen is reduced to water with electrons donated from NADH and $FADH_2$ (Nelson and Cox, 2005). The high energy electrons are transferred exergonically by a series of membrane-bound electron carriers, and the free energy which is generated is coupled to the transfer of protons across an impermeable membrane to an area of higher concentration (Nelson and Cox, 2005). This generates an electro-chemical potential. Protons flow across the membrane down the concentration gradient through ATP synthase, a membrane protein that couples proton flow to phosphorylation of ADP (Nelson and Cox, 2005).

F_1-ATPase has six nucleotide binding sites on the α/β hexamer; three are catalytic and three are non-catalytic (Bald *et al.*, 1998). Each of these sites is located on the interface between α and β. ATP, ADP, and Pi bind at the βTP, βDP, and βE sites respectively. Boyer (1979) proposed a 'binding change mechanism' for the binding of ATP, ADP, and Pi in which each catalytic site changes to bind/release the products and substrates. Clockwise rotation of asymmetric γ, as viewed looking up from the membrane, results in synthesis of ATP, and hydrolysis occurs during the anti-clockwise rotation. This was shown in the single particle experiments of Itoh's group (Cabezon, *et*

al., 2003; Itoh *et al.*, 2004; Noji *et al.*, 1997).

As protons flow through the *c* subunit, the γ subunit rotates creating conformational changes within the β subunit. For every 120° rotation, one ATP is synthesized: three ATP per 360° (Nakamoto *et al.*, 2008). In theory, if one proton is carried per *c* subunit, and three ATP are generated per 360° rotation, then the number of ions transported during one full rotation equals the number of *c* subunits (Nakamoto *et al.*, 2008). The number of ions transported divided by three provides the stoichiometry of ions required for ATP catalysis (Nakamoto *et al.*, 2008).

The 120° rotations can be broken down into two partial rotations of 80° and 40°. Before each 80° rotation there is a short dwell which is believed to be the rate limiting step when ATP binds. The duration of the dwell is ATP-dependent and determines the rate of ATPase activity. In the reverse direction, ATP synthesis, the 40° rotation creates a high affinity for P_i, and the following 80° rotation reduces the affinity for ATP which allows the molecule to be released. ATP release and P_i binding are the energy requiring steps during catalysis (Nakamoto *et al.*, 2008). Al-Shawi *et al.* (1990) postulated that the energy gained from binding P_i and the release of ATP during substrate-protein interactions is the driving force behind catalysis (Al-Shawi *et al.*, 1990; Nakamoto *et al.*, 2008). The importance of P_i binding is discussed in more detail below in the Modulation section.

Human Health and Disease

ATP plays a role in metabolic pathways within the cell and has implications in many diseases (Dadi *et al.,* 2009; Hong and Pedersen, 2008). For instance, mutation(s) in any one of the subunits of ATP synthase may cause Leigh syndrome, or a resistance to

darylquinoline, a new Tuberculosis drug (Andries *et al.*, 2005; Cole and Alzari, 2005; Hong and Pedersen, 2008). Mitochondrial DNA-associated Leigh syndrome is part of a continuum of progressive neurodegenerative disorders caused by abnormalities of mitochondrial energy generation (Thorburn and Rahman, 2006). Neurodegenerative processes in Alzheimer's disease have been associated with the accumulation of α subunits in the intraneuronal cytosol (Schagger and Ohm, 1995).

Common diseases such as obesity and high blood pressure have been correlated with ATP synthase as well (Hong and Pedersen, 2008). Increases in blood pressure have been correlated with increased F_6 circulating in the blood (Hong and Pedersen, 2008). When non-mitochondrial ATP synthase is inhibited, cytosolic lipid droplet accumulation decreased, implying ATP synthase as a potential anti-obesity drug target (Hong and Pedersen, 2008).

Other diseases such as mitochondrial myopathies, Parkinson's, and cancer are correlated with ATP synthase (Hong and Pedersen, 2008). A thorough review of mitochondrial pathology and the genetics of mitochondrial diseases can be found in Wallace (1999). A few diseases mentioned in the review that are associated with genetic disorders are Leber's hereditary optic neuropathy (LHON), dystonia, Leigh's disease, Kearns-Sayre Syndrome (KSS), autosomal dominant-progressive external ophthalmoplegia (AD-PEO), mtDNA depletion syndrome, mitochondrial neurogastrointestinal encephalopathy syndrome (MNGIE), and Huntington's disease (Wallace, 1999).

ATP synthase has been found on the extracellular surface of endothelial cells, a variety of cancer cells, and on neuronal cells (Chi and Pizzo, 2006; Xing *et al.*, 2010). In

the case of tumor cells, the blocking of angiogenesis through reaction of inhibitors with non-mitochondrial ATP synthase has been shown: angiostatin has been shown to be antitumorigenic, and the β subunit is a target protein for innate antitumor cytotoxicity through the action of natural killer and interleukin 2-activated killer cells (Chi and Pizzo, 2006; Gledhill *et al.,* 2007; Hong and Pedersen, 2008). In such cases ATP synthase could be a molecular target for various therapies. There is no telling what the future may hold for cancer therapies. Perhaps one day, lymphocytes could be grown, harvested, and directed towards the site of tumor growth, or various β subunit inhibitors could be injected at a tumor site in order to slow growth or reduce the size of a tumor without surgical invasion. A thorough review of ATP synthase inhibitors can be found in Hong and Pedersen (2008).

Understanding the role of ATP synthase in human disease conditions is imperative, but ATP synthase serves important roles in other organisms too. For example, in insects juvenile hormone (JH) is responsible for reproductive development and metamorphosis. As an insect matures the levels of JH drop off (Zalewska *et al.*, 2009). By exposing larvae to JH, they are unable to develop further and they remain in the larval state (Zalewska *et al.*, 2009). This knowledge is used in agriculture: methoprene, a synthetic JH, is an insect growth regulator and is used to prevent the reproductive development of pest insects such as mosquitoes and insects in the orders Diptera, Lepidoptera, and Coleoptera (Csondes, 2004).

Juvenile hormone, JH, needs to be transported to various cells in order to have an effect on development, and most of the time the hormone is bound by a protein known as juvenile hormone binding protein (JHBP) (Zalewska *et al.*, 2009). ATP synthase has

been identified as a JHBP-binding protein, and it was shown that ATP synthase is involved with transport of JHBP out of a cell (Zalewska *et al.*, 2009). The JHBP-JH complex will not bind to ATP synthase (Zalewska *et al.*, 2009).

The crystal structure of JHBP from *Galleria mellonella* shows an unusual fold consisting of a long α-helix wrapped in a highly curved antiparallel β-sheet (Kolodziejczyk *et al.*, 2008). JHBP structurally resembles the folding pattern found in tandem repeats in some mammalian lipid-binding proteins, with similar organization of one cavity and a disulfide bond between the long helix and the β-sheet (Kolodziejczyk *et al.*, 2008). Therefore, JHBP has an archetypal fold used by nature for hydrophobic ligand binding (Kolodziejczyk *et al.*, 2008). With structural and functional similarity between JHBP and mammalian lipid binding proteins, could there be an underlying medicinal application for understanding JHBP and its interactions with ATP synthase? Perhaps by simply understanding the JHBP and ATP synthase protein-protein interactions we may come to understand more about bactericidal/permeability-increasing protein (BPI) and cholesteryl ester transfer protein (CETP), two mammalian lipid binding proteins (Zalewska *et al.*, 2009).

BPI is correlated with Chron's disease and ulcerative colitis which are both inflammatory bowel diseases (Petermann *et al.*, 2009). It was shown that upon addition of BPI, the β-subunit of the F_1 portion of *Escherichia coli* ATP synthase was repressed threefold (Qi *et al.*, 1995). This shows that one mode of BPI's antimicrobial action is through the suppression of metabolic processes (Qi *et al.*, 1995).

Plasma HDL is a negative risk factor for atherosclerosis (Takahashi *et al.*, 1993). Cholesteryl ester transfer protein (CETP) transfers cholesteryl ester from HDL to other

lipoproteins (Takahashi *et al.*, 1993). Defects in CETP are associated with increased HDL cholesterol levels which are inversely correlated with risk of coronary artery disease (Takahashi *et al.*, 1993). Zhang *et al.* (2008) explored the effects of niacin on the surface expression of ATP synthase β chain, a newly described HDL/apolipoprotein A-I receptor for HDL endocytosis in HepG2 cells. In their article Zhang *et al.* (2008) showed that α and β ATP synthase chains are specifically expressed on the cell surface of hepatocytes, endothelial cells, lymphocytes, and some tumor cell lines but not on the CHO cell line (Zhang *et al.,* 2008). Although the reason for expression on these specific cell types is not thoroughly understood, it may be involved in angiogenesis, hypertension, cell proliferation, and cytotoxicity in addition to HDL endocytosis (Zhang *et al.,* 2008).

Not only do the protein-protein interactions of ATP synthase and lipid binding proteins need to be understood on the cellular level, but these interactions must be understood from the genetic level in order for us to obtain a solid understanding of when and how these interactions are occurring, and what regulatory pathways are being involved during protein-protein interactions. Defects in CETP have been associated with higher levels of HDL cholesterol. Understanding the genetic basis for these defects may provide insight in targeting normal CETP or altering it to the defective form through gene therapy in order to benefit individuals with low levels of HDL cholesterol. Using the arthropod system for research would provide an inexpensive means for understanding more about the role of ATP synthase in binding lipid binding proteins.

Beyond using ATP synthase for a drug target or pharmaceutical development, we can use it as a prototype for a nanomotor. ATP synthase exists in the body, interacting with any number of proteins and other molecules at any given time, so why not use this

enzyme as a base model to develop a tiny machine that can go inside our bodies to perform various types of work?

Nanomedicine, an offshoot of nanotechnology, refers to highly specific medical interventions on the molecular scale for curing disease or repairing damaged tissues (http://nihroadmap.nih.gov/nanomedicine/). Unclogging arteries, fighting infections, or helping to monitor body systems are a few things nanomachines might be capable of. But once a nanomachine is inside the body, how big can it be? How fast can it work? Can we alter its speed? How many can we have to perform efficiently without disrupting homeostasis? These questions must be addressed in order to build nanomachines that are compatible with living tissues and can safely operate inside the body (Ahmad and Senior, 2005a; Whitesides, 2003; http://nihroadmap.nih.gov/nanomedicine/).

Currently, ATP synthase is the smallest known biological nanomotor. Therefore, understanding the mechanisms of how this enzyme works and using ATP synthase as a base model may help to develop nanomotors for nanomedicine usage. This, of course, is the ultimate goal of our research. For that reason, we focus on characterizing the catalytic sites of ATP synthase to find out which residues are responsible for binding inorganic phosphate (P_i), thus driving the synthesis of cellular ATP.

Modulation

Through mutagenic analysis, it is possible characterize individual residues, specifically within the α/β-catalytic sites. Eight residues in close proximity to the catalytic site have been studied, and it was found that five residues (βArg-246, αArg-376, βLys-155, βArg-182, and αSer-347) are responsible for binding P_i, a determining factor in the synthesis of ATP (Ahmad and Senior, 2004a, 2005b, 2006; Li *et al.,* 2009); and

three residues (βAsn-243, βPhe-291, and αGly-351) were found to be important for overall function but not in P_i binding (Ahmad and Senior, 2004b; Brudecki *et al.*, 2008; Li *et al.*, 2009).

The five residues responsible for P_i binding are within the phosphate-binding subdomain and are positioned in a triangular fashion. The X-ray crystal structures of bovine ATP synthase show a sequence of residues that reside along the top of the triangular catalytic site: αVal-345, αIle-346, αSer-347, αIle-348, αThr349, αAsp350, and αGly-351. These residues have been conserved throughout evolution and are known as the α subunit VISIT-DG sequence residues (Li *et al.*, 2009). VISIT-DG sequence residues may potentially be essential for P_i binding. αSer-347 of the VISIT-DG sequence was the fifth residue recently found to be important for P_i binding (Li *et al.,* 2009). However, αGly-351 has also been investigated for its role in P_i binding but was shown to play an indirect role (Li *et al.*, 2009).

For the work discussed herein, experiments were designed to test the hypothesis that other residues in this highly conserved region are important for P_i binding. Specifically, we asked if αThr-349 is directly involved in P_i binding: αThr-349 contains a hydroxyl side chain oriented towards the P_i binding cavity and may have a similar function to that of αSer-347. Is the hydroxyl group on the side chain of αThr-349 involved in charge communication with βArg-182 or important for transition state?

In order to investigate the role of αThr-349, or other VISIT-DG residues, site-directed mutagenesis can be employed. Base pair mutations of various residues to alanine, aspartic acid, and arginine are helpful as they show how the native amino acid residue's side chain size and/or charge affect catalysis.

For example, alanine has a non-polar, neutral side chain which consists only of a methyl group (Fig. 1.2). By replacing Thr with Ala, it is possible to test whether or not the hydroxyl group on the side chain of Thr is important for P_i binding. As shown in Figure 1.2, aspartic acid has a negatively charged side chain. By introducing Asp at position 349 in place of Thr we will be able to determine if Thr maintains some sort of structural integrity. Arginine is a large, polar molecule with a positively charged side chain (Fig. 1.2). By inserting a positive charge in place of threonine, will P_i binding be enhanced by the additional positive charge? Or will there be charge repulsion between the inserted arginine and the nearby βArg-182, a known P_i binding residue, which might result in loss of structural integrity and P_i binding elimination? If this mutation is coupled with removing the positive charge of βR182, will αT349R compensate for the loss of βR182?

There is a multitude of combinations that can be created in mutational studies. Once a residue of interest is chosen, mutant strains can be constructed using the logic above. Then, each mutant strain must undergo a series of biochemical assays to determine what, if any, effect the mutation has and a role for the original amino acid residue is postulated.

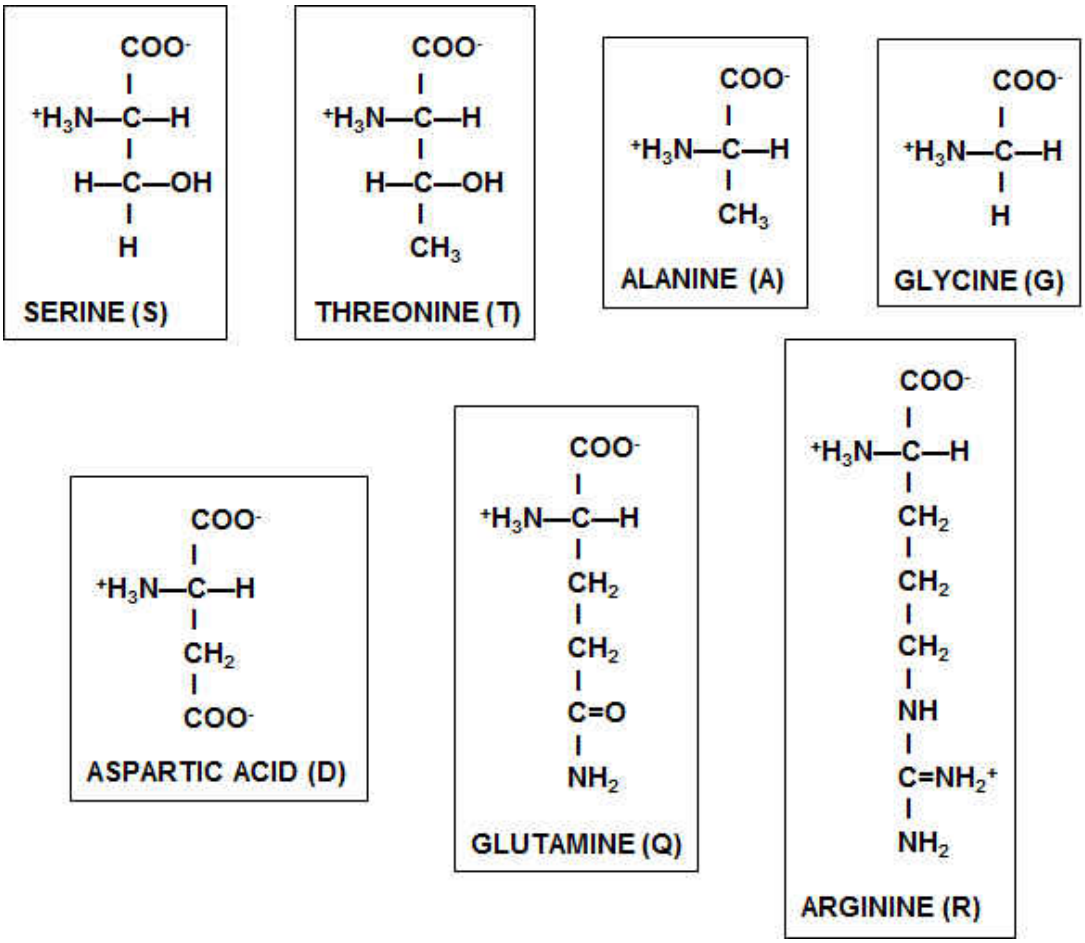

FIGURE 1.2 **Structure of amino acid residues.** The structure, name, and one letter symbol for serine, threonine, glycine, alanine, aspartic acid, glutamine, and arginine are shown from left to right, top to bottom.

Further characterization of function of mutant proteins involves testing how the ability to bind inhibitors is affected by the mutation. ATP synthase activity can be inhibited by a multitude of compounds that can bind various locations on any one subunit. The F_O portion is named so for its oligomycin sensitivity-conferring protein (OSCP) (Hong and Pedersen, 2008). The F_1 subunit has binding sites for basic α-helical peptide inhibitors such as IF_1 and melittin (Hong and Pedersen, 2008). Hong and Pedersen's review (2008) discusses the action of inhibitors such as polyphenolic phytochemicals, polyketides, organotins, cations, substrate analogs, amino acid

modifiers, and other compounds on ATPase activity, as well as physical inhibition of activity by high hydrostatic pressure, low temperature, and UV irradiation. Knowledge of inhibitor binding sites coupled with biochemical assays on mutant enzymes provides insight into how specific amino acids are contributing to the binding of various inhibitors.

Overall, this work will lead to a more thorough understanding of what residues are essential for binding P_i. This knowledge will provide groundwork on which modulation of ATP synthase can be achieved and applied in the field of nanotechnology.

CHAPTER 2

ROLE OF α-SUBUNIT VISIT-DG SEQUENCE RESIDUES SER-347 AND GLY-351 IN THE CATALYTIC SITES OF *ESCHERICHIA COLI* ATP SYNTHASE*

Wenzong Li[‡], Laura E. Brudecki[‡], Alan E. Senior[§], and Zulfiqar Ahmad[‡1]

[‡]Department of Biological Sciences, East Tennessee State University, Johnson City, Tennessee 37614

[§]Department of Biochemistry and Biophysics, University of Rochester Medical Center, Rochester, New York 14642

[1]To whom correspondence should be addressed: Dept. of Biological Sciences, Box 70703, East Tennessee State University, Johnson City, TN 37614. Tel.: 423-439-6931; Fax: 423-439-5958; E-mail: ahmadz@etsu.edu.

"This research was originally published in The Journal of Biological Chemistry. Li, W., Brudecki, L.E., Senior, A.E., and Ahmad, Z. Role of α-Subunit VISIT-DG Sequence Residues Ser-347 and Gly-351 in the Catalytic Sites of *Escherichia coli* ATP Synthase. *J Biol Chem*. 2009; 284:10747-10754. © the American Society for Biochemistry and Molecular Biology."

Abstract

This paper describes the role of α-subunit VISIT-DG sequence residues αSer-347 and αGly-351 in catalytic sites of *Escherichia coli* F_1F_o ATP synthase. X-ray structures show the very highly conserved α-subunit VISIT-DG sequence in close proximity to the conserved phosphate-binding residues αArg-376, βArg-182, βLys-155, and βArg-246 in the phosphate-binding subdomain. Mutations αS347Q and αG351Q caused loss of oxidative phosphorylation and reduced ATPase activity of F_1F_o in membranes by 100- and 150-fold, respectively, whereas αS347A mutation showed only a 13-fold loss of activity and also retained some oxidative phosphorylation activity. The ATPase of αS347Q mutant was not inhibited, and the αS347A mutant was slightly inhibited by MgADP-azide, MgADP-fluoroaluminate, or MgADP-fluoroscandium, in contrast to wild type and αG351Q mutant. Whereas 7-chloro-4-nitrobenzo-2-oxa-1, 3-diazole (NBD-Cl) inhibited wild type and αG351Q mutant ATPase essentially completely, ATPase in αS347A or αS347Q mutant was inhibited maximally by ~80–90%, although reaction still occurred at residue βTyr-297, proximal to the α-subunit VISIT-DG sequence, near the phosphate-binding pocket. Inhibition characteristics supported the conclusion that NBD-Cl reacts inβE (empty) catalytic sites, as shown previously by x-ray structure analysis. Phosphate protected against NBD-Cl inhibition in wild type and αG351Q mutant but not in αS347Q or αS347A mutant. The results demonstrate that αSer-347 is an additional residue involved in phosphate-binding and transition state stabilization in ATP synthase catalytic sites. In contrast, αGly-351, although strongly conserved and clearly important for function, appears not to play a direct role.

Introduction

F_1F_o-ATP synthase is the enzyme responsible for ATP synthesis by oxidative or photophosphorylation in membranes of bacteria, mitochondria, and chloroplasts. It is the fundamental means of cell energy production in animals, plants, and almost all microorganisms. It works like a nanomotor and is structurally similar in all species. In its simplest form, as in *Escherichia coli*, it contains eight different subunits distributed in the water-soluble F_1 sector (subunits $\alpha_3\beta_3\gamma\delta\varepsilon$) and the membrane-associated F_o sector (subunits ab_2c_{10}). The total molecular size is ~530 kDa. In chloroplasts there are two isoforms of subunit *b*. In mitochondria, there are 7–9 additional subunits, depending on the source, but *in toto* they contribute only a small fraction of additional mass and may have regulatory roles (1–4).

ATP hydrolysis and synthesis occur in the F_1 sector. X-ray structures of bovine enzyme (5) established the presence of three catalytic sites at α/β subunit interfaces of the $\alpha_3\beta_3$ hexamer. Proton transport occurs through the membrane-embedded F_o. The γ-subunit contains three α-helices. Two of these helices form a coiled coil and are located in the central space of the $\alpha_3\beta_3$ hexamer. Proton gradient-driven clockwise rotation of γ (as viewed from the membrane) leads to ATP synthesis and anticlockwise rotation of γ results from ATP hydrolysis. In recent terminology, the rotor consists of $\gamma\varepsilon c_n$, and the stator consists of $b_2\delta$ (6, 7). The function of the stator is to prevent co-rotation of catalytic sites with the rotor. Detailed reviews of ATP synthase structure and function may be found in Refs. 8–13.

To better understand the reaction mechanism of ATP synthesis and hydrolysis and

their relationship to mechanical rotation in this biological nanomotor, we have focused our efforts on determining the role of conserved residues in and around catalytic site P_i-binding subdomain. Knowledge of P_i-binding residues and residues surrounding the P_i-binding subdomain is imperative for accomplishing (i) the molecular modulation of the catalytic site for the improved catalytic and motor function of this enzyme, (ii) an explanation of how ATP synthase binds ADP and P_i within its catalytic sites in the face of a relatively high ATP/ADP concentration ratio, and (iii) understanding the relationship between P_i binding and subunit rotation (14–16). Earlier attempts to measure P_i binding in purified *E. coli* F_1 using [^{32}P]P_i (15) or by competition with ATP or AMP-PNP[2] in fluorescence assays of nucleotide binding (18, 19) failed to detect appreciable P_i binding at physiological P_i concentration. So, we turned to the assay devised by Perez *et al.* (20) in which the protection afforded by P_i against inhibition of ATPase activity induced by covalent reaction with 7-chloro-4-nitrobenzo-2-oxa-1, 3,-diazole (NBD-Cl) provides the measure of P_i binding. Earlier Orriss *et al.* (21) showed by x-ray crystallography that the covalent adduct formed by NBD-Cl is specifically in the βE catalytic site (Fig. 2.1*A*); thus protection afforded by P_i indicates that binding of P_i occurs at the βE catalytic site. By modifying the above assay for use with *E. coli* purified F_1 or F_1F_o membranes, we have previously investigated the relationship between P_i binding and catalysis for six residues, namely βArg-246, βAsn-243, αArg-376, βLys-155, βArg-182, and αPhe-291.[3] All of these residues are positioned in proximity to the phosphate analogs AlF_3 or SO_4^{2-} in x-ray structures of catalytic sites (22, 23). We found that four residues, namely βArg-246, αArg-376, βLys-155, and βArg-182, grouped in a triangular fashion are directly involved in P_i binding (Fig. 2.1*B*) (24–30).

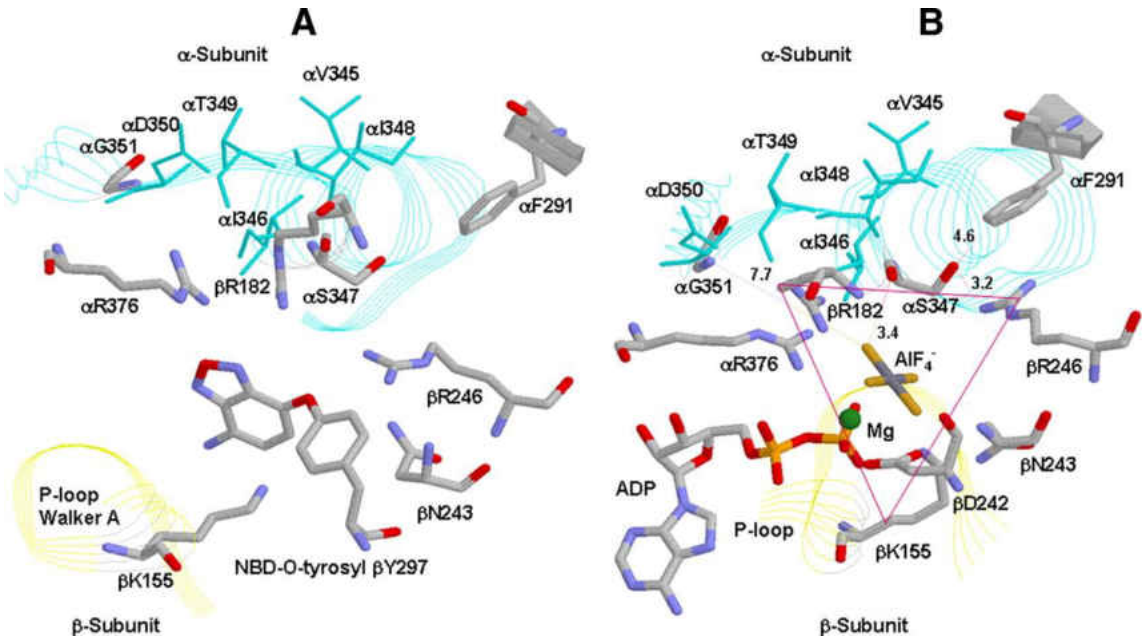

FIGURE 2.1. **X-ray structures of catalytic sites in mitochondrial ATP synthase showing spatial relationship of α-subunit VISIT-DG sequence αS347 and αG351.** *A*, reacted NBD-O-tyrosyl-297 in the βE site (21). *B*, the βDP site in the AlF_4^- inhibited enzyme (23). *E. coli* residue numbering is shown. The *triangle* shows the residues βLys-155, βArg-182, βArg-246, αArg-376, and αSer-347 forming a triangular P_i-binding site. Rasmol software was used to generate these figures.

It is interesting to note that Penefsky (31) detected [^{32}P] P_i binding with a K_d (P_i) in the range of 0.1 mM in mitochondrial membranes using a pressure ultrafiltration method, and the results are in agreement with data obtained from the NBD-Cl protection assay (20). However, Penefsky could not detect P_i binding in *E. coli* F_1F_o, and thus it is evident that P_i dissociates more rapidly from *E. coli* F_1 than it does from mitochondrial F_1. This unfortunately renders the potentially more convenient centrifuge column assay unsuitable with the *E. coli* enzyme.

A mechanism of condensation of P_i with MgADP was proposed by Senior *et al.* (32). The x-ray crystallography structure of bovine ATP synthase by Menz *et al.* (23) shows the transition state analog MgADP-AlF_4^- trapped in catalytic sites (Fig. 2.1*B*). It is clear from the geometry of this complex that the fluoroaluminate group occupies the

position of the ATP-γ-phosphate in the predicted transition state. Similarly, Pedersen and co-workers (33) reported the first transition state-like structure of F_1 using enzyme obtained from rat liver and crystallized with the P_i analog vanadate (V_i). This work further demonstrated that ADP was not essential, suggesting that the MgVi-F_1 complex inhibited the catalytic activity to the same extent as that observed for the MgADP-Vi-F_1 complex. Unfortunately, neither MgVi nor MgADP-Vi inhibits the *E. coli* enzyme (24). Thus we have relied on inhibition of ATPase activity by fluoroaluminate (or fluoroscandium) to assess the potential to stabilize a transition state complex (24–26, 28, 30). Through mutagenesis and by employing the NBD-Cl protection assay as well as ATPase inhibition by transition state analogs, we can probe the direct or indirect role of residues in P_i binding. In this manuscript, we explore the possible role played by αSer-347 and αGly-351 residues in the highly conserved α-subunit VISIT-DG sequence. Fig. 2.1*B* shows the location of αSer-347 and αGly-351 residues. Notably, αSer-347 appears to occupy a strategic position in the P_i-binding subdomain. Fig. 2.2 shows the evolutionarily conserved α-subunit VISIT-DG sequence along with surrounding residues of α-subunit from a variety of species. The basic questions we asked were: what role does αSer-347 or αGly-351 play? Do the mutations αS347A, αS347Q, or αG351Q have any effect on P_i binding or transition state formation?

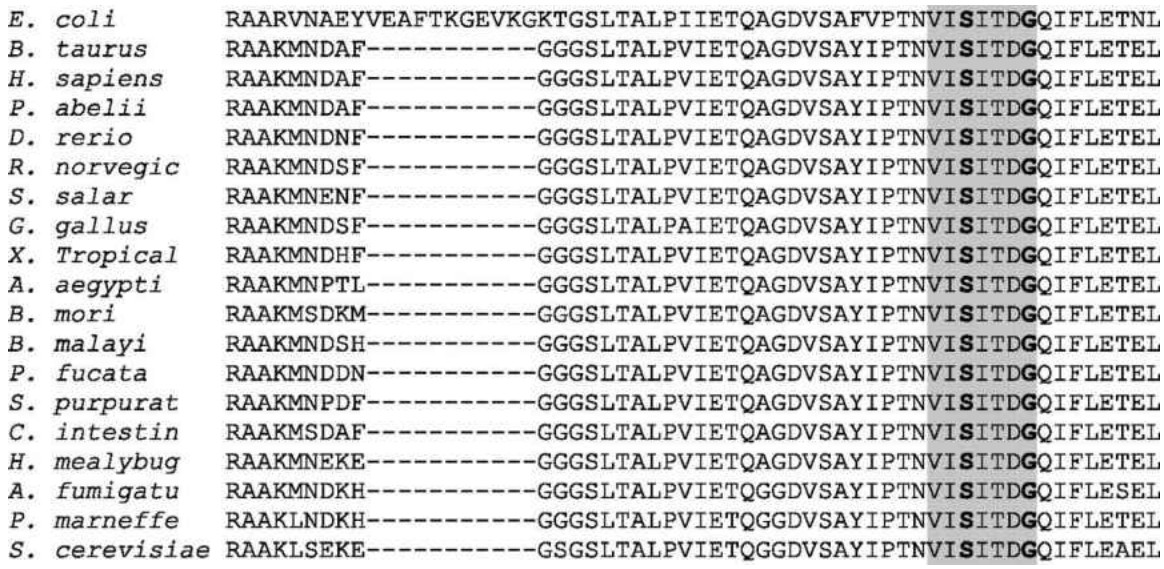

FIGURE 2.2. **Amino acid sequence alignment of evolutionarily conserved α-subunit VISIT-DG sequence.** α-Subunit sequence from different species is aligned. The highly conserved VISIT-DG sequence is highlighted in *gray*. The starting residue arginine shown here for *E. coli* is αR300. Conserved αSer-347 and αGly-351 are denoted by bold font.

Materials and Methods

Construction of Wild Type and Mutant Strains of E. coli—The wild type strain was pBWU13.4/DK8 (34). Mutagenesis was by the method of Vandeyar *et al.* (35). The template for oligonucleotide-directed mutagenesis was M13mp18 containing the HindIII-XbaI fragment from pSN6. pSN6 is a plasmid containing the βY331W mutation from plasmid pSWM4 (36) introduced on a SacI-EagI fragment into pBWU13.4 (34), which expresses all the ATP synthase genes. pSWM67/AN888 strain was used for αS347A mutant (37). The mutagenic oligonucleotide for αS347Q was CCAACGTAATCCAGATTACCGATGG, where the underlined bases introduce the mutation and a new XcmI restriction site, and that for αG351Q was CCATTACCGATCAGCAAATCTTCCTGGAAACC, where the underlined bases introduce the mutation and a silent mutation removes BglII restriction site. DNA sequencing was performed to confirm the presence of mutations and absence of undesired

changes in sequence, and the mutations were transferred to pSN6 on a Csp451 (an isoschizomer of BstBI) and Pml1 fragment generating the new plasmids pZA13 (αS347Q/βY331W) and pZA14 (αG351Q/βY331W). Each plasmid was transformed into strain DK8 (38) containing a deletion of ATP synthase genes for expression of the mutant enzymes. It may be noted that both mutant strains contained the βY331W mutation, which is valuable for measurement of nucleotide binding parameters (36) and does not affect function significantly on its own. Although the presence of βY331W mutation was not utilized in this work, the Trp mutation was included for possible future use.

Preparation of E. coli Membranes, Measurement of Growth Yield in Limiting Glucose Medium, and Assay of ATPase Activity of Membranes—E. coli membranes were prepared as in Ref. 39. It should be noted that this procedure involves three washes of the initial membrane pellets. The first wash is performed in buffer containing 50 mM TES, pH 7.0, 15% glycerol, 40 mM 6-aminohexanoic acid, 5 mM *p*-aminobenzamidine. The following two washes are performed in buffer containing 5 mM TES, pH 7.0, 15% glycerol, 40 mM 6-aminohexanoic acid, 5 mM *p*-aminobenzamidine, 0.5 mM DTT, 0.5 mM EDTA. Prior to the experiments, the membranes were washed twice more by resuspension and ultracentrifugation in 50 mM $TrisSO_4$, pH 8.0, 2.5 mM $MgSO_4$. Growth yield in limiting glucose was measured as in Ref. 40. ATPase activity was measured in 1 ml of assay buffer containing 10 mM NaATP, 4 mM $MgCl_2$, 50 mM $TrisSO_4$, pH 8.5, at 37 °C. The reactions were started by the addition of membranes and stopped by the addition of SDS to 3.3% final concentration. P_i released was assayed as in Ref. 41. For wild type membranes (20–30 μg of protein), reaction times were 5–10 min. For mutant membranes (40–60 μg of protein), reaction times were 30–50 min. All of the reactions

were shown to be linear with time and protein concentration. SDS gel electrophoresis on 10% acrylamide gels was as in Ref. 42. Immunoblotting with rabbit polyclonal anti-F_1-α and anti-F_1-β antibodies was as in Ref. 43.

Inhibition of ATPase Activity by NBD-Cl and Protection by MgADP or P_i—NBD-Cl was prepared as a stock solution in dimethyl sulfoxide and protected from light. The membranes (0.2–0.5 mg/ml) were reacted with NBD-Cl for 60 min in the dark at room temperature in 50 mM TrisSO_4, pH 8.0, 2.5 mM $MgSO_4$, and then 50-μl aliquots were transferred to 1 ml of ATPase assay buffer to determine ATPase activity. Where protection from NBD-Cl inhibition by ADP or P_i was determined, the membranes were preincubated 60 min with protecting agent at room temperature before the addition of NBD-Cl. $MgSO_4$ was present, equimolar with ADP or P_i. Control samples containing the ligand without added NBD-Cl were included. Neither P_i (up to 50 mM) nor MgADP (up to 10 mM) had any inhibitory effect alone.

Reversal of NBD-Cl Inhibited ATPase Activity by DTT—For reversal of NBD-Cl inhibition by DTT, the membranes were first reacted with NBD-Cl (150 μM) for 1 h at room temperature, and then DTT (final = 4 mM) was added, and incubation continued for 1 h at room temperature before ATPase assay. Control samples without NBD-Cl and/or DTT were incubated for the same times.

Inhibition of ATPase Activity by Azide, Fluoroaluminate, or Fluoroscandium—Azide inhibition was measured by preincubating membranes with varied concentrations of sodium azide for 30 min. Then 1 ml of ATPase assay buffer was added to measure the activity. For measurements of fluoroaluminate or fluoroscandium inhibition, the

membranes were incubated for 60 min at room temperature in 50 mM $TrisSO_4$, 2.5 mM $MgSO_4$, 1 mM NaADP, and 10 mM NaF at a protein concentration of 0.2–0.5 mg/ml in presence of $AlCl_3$ or $ScCl_3$ added at varied concentration (see "Results"). 50-µl aliquots were then added to 1 ml of ATPase assay buffer, and activity was measured as above. It was confirmed in control experiments that no inhibition was seen if $MgSO_4$, NaADP, or NaF was omitted.

Inhibition of ATPase Activity by Dicyclohexylcarbodiimide (DCCD)—Covalent modification of wild type and mutant membrane was performed as described by Weber *et al.* (44). ATPase activity was measured by adding 1 ml of ATPase assay buffer containing 10 mM NaATP, 4 mM $MgCl_2$, 50 mM $TrisSO_4$, pH 8.5, at 37 °C to the 100-µl aliquots of 16 h DCCD-modified ATP synthase.

Results

Growth Properties of α*S347Q,* α*S347A, and* α*G351Q Mutants of E. coli ATP Synthase*—Three new mutants, αS347Q, αS347A, and αG351Q, were generated. These two residues were chosen for mutagenesis because of their strong conservation in the α-subunit VISIT-DG sequence and their close proximity to the P_i-binding pocket. The αS347A mutant was used to appreciate the role of Ser-OH side chain in P_i binding and transition state. αS347Q and αG351Q mutants were designed to understand the impact of larger side chain of Gln on αSer-347 and αGly-351.

Table 2.1 shows that introduction of Gln as αS347Q and αG351Q resulted in the loss of oxidative phosphorylation. Both mutations prevented growth on succinate-containing medium, and growth yields in limiting glucose medium were reduced close to

those of the ATP synthase null control. αS347A mutant, on the other hand, resulted in partial loss of oxidative phosphorylation. Specific ATPase activities of membrane preparations containing mutant enzymes were compared with wild type and null control, and the values are shown in Table 2.1. αS347Q and αG351Q reduced the ATPase activity by 100–150-fold, whereas ATPase activity was reduced only 13-fold by αS347A. Membranes prepared from the mutants contained the same amount of α and β subunits as wild type, as determined by SDS gel electrophoresis and immunoblotting (26) (data not shown); therefore, reduced ATPase is not due to impaired assembly of ATP synthase or loss of F_1 during membrane preparation.

TABLE 2.1 **Effects of αSer-347 and αGly-351 mutation on cell growth and ATPase activity**

Mutation[a]	**Growth on succinate**[b]	**Growth yield in limiting glucose**	**ATPase activity**[c]
		%	*μmol/min/mg*
Wild type	++++	100	28
Null	–	46	0
βY331W	++++	95	26
αS347Q	±	55	0.20
αS347A	+	65	2.18
αG351Q	±	54	0.25

[a] Wild type, pBWU13.4/DK8; Null, pUC118/DK8, αS347Q/DK8, αG351Q/DK8, and αS347A/AN888. Both αS347Q and αG351Q mutants were expressed with the βY331W mutation also present, which does not significantly affect growth. The data are the means of four to six experiments each.

[b] Growth on succinate plates after 3 days estimated by eye. ++++, heavy growth; +, partial growth; ±, very light growth; –, no growth.

[c] ATPase activity was measured at 37°C and expressed as μmol of ATP hydrolyzed/min/mg of membrane protein. Each individual experimental point is itself the mean of duplicate assay tubes. The data are derived from two separate membrane preparations. The results from separate membrane preparations were in excellent agreement within ± 10%.

Inhibition of ATPase Activity of ATP Synthase in Membranes by NBD-Cl and Reversal by Dithiothreitol—We previously established that P_i binding by mutant or wild type ATP synthase can be assayed using either membrane preparations or purified F_1, with equivalent results (24, 26). In this work we used membrane preparations that are more convenient. Fig. 2.3 shows NBD-Cl inhibition of wild type and mutant membranes in the presence of varied concentrations of NBD-Cl. In wild type potent inhibition occurred with no residual activity, and this is consistent with previous studies (24–28, 30). αG351Q mutant was also completely inhibited, and αS347Q or αS347A mutant were inhibited by ~80–90% with ~20–10% residual activity. In previous studies (24–28, 30), we have noted several instances where mutant ATP synthases were incompletely inhibited by NBD-Cl. To be sure that maximal reaction with NBD-Cl had been reached, we incubated each membrane preparation with 150 μM NBD-Cl for 1 h as in Fig. 2.3, followed by an additional pulse of 200 μM NBD-Cl, continuing the incubation for an additional hour before assaying ATPase activity. Very little or no additional inhibition occurred (Fig. 2.4, *left panel*). This shows that the reaction of NBD-Cl was complete and that fully reacted αS347Q mutant membranes retained residual activity. Next, we checked whether inactivation by NBD-Cl could be reversed by the addition of the reducing agent DTT because reversibility by DTT was indicative of specificity of reaction in previous studies. Wild type and mutant enzymes were preincubated with 150 μM NBD-Cl as in Fig. 2.3, and then 4 mM DTT was added, and incubation continued for 1 h before ATPase assay. It was seen that DTT completely restored full activity in all cases (Fig. 2.4, *right panel*). This indicates that NBD-Cl reacts specifically with residue βTyr-297 in the wild type as well as in both mutants (45, 46).

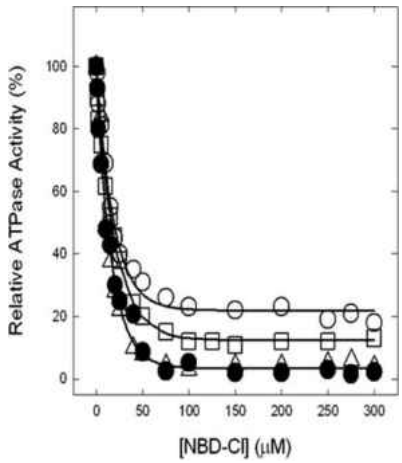

FIGURE 2.3. **Inhibition of membrane-bound wild type and mutant ATP synthase by NBD-Cl.** The membranes were preincubated for 60 min at room temperature with varied concentration of NBD-Cl, and then aliquots added to 1 ml of assay buffer and ATPase activity were determined. The details are given under "Materials and Methods." ●, wild type; ○, αS347A; □, αS347Q; Δ, αG351Q. Each data point represents an average of at least four experiments, using two independent membrane preparations of each mutant. The results agreed within ±10%.

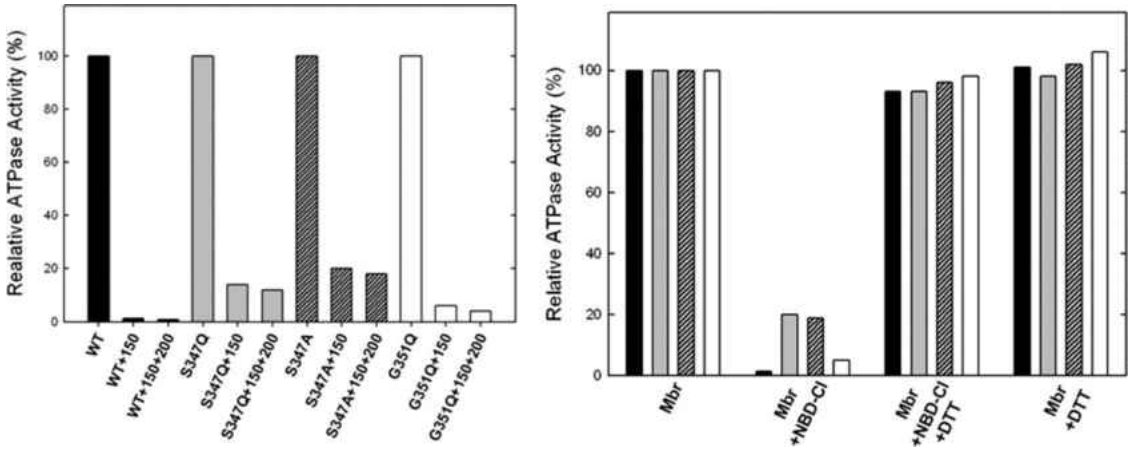

FIGURE 2.4. **Results of extra pulse of NBD-Cl in mutants and reversal of NBD-Cl effects by DTT.** *Left panel*, membrane ATP synthase was inhibited with 150 μM NBD-Cl for 60 min under conditions as described in Fig. 2.3. Then a further pulse of 200 μM NBD-Cl was added, and incubation continued for 1 h before assay. *Right panel*, membrane ATP synthase *(Mbr*) was incubated with or without 150 μM NBD-Cl for 60 min under conditions as described for Fig. 2.3. The degree of inhibition was assayed. In parallel samples, 4 mM DTT was then added, and incubation continued for further 60 min before assay. Each set of bars represents wild type, αS347Q, αS347A, and αG351Q from *left* to *right*. The absolute residual ATPase activity values are as follows: wild type, 28, 0.36, 0.22; αS347Q, 0.20, 0.03, 0.02; αS347A, 2.18, 0.44, 0.39; and αG351Q, 0.25, 0.02, 0.01.

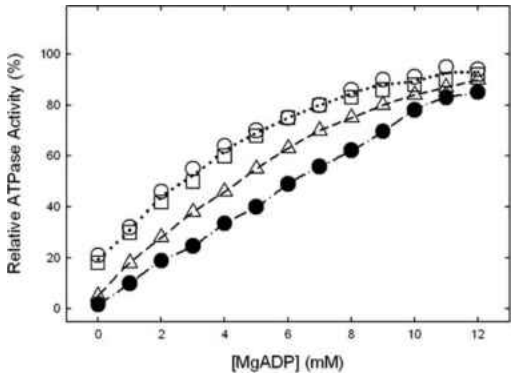

FIGURE 2.5. **Protection against NBD-Cl reaction by MgADP.** Wild type and mutant membrane were preincubated for 1 h at room temperature with varied concentrations of MgADP as shown, then 150 μM NBD-Cl was added, and incubation continued at room temperature in the dark for 1 h. The aliquots were then assayed for ATPase activity. ●, wild type; ○, αS347A; □, αS347Q; Δ, αG351Q. The results are the means of quadruplicate experiments which agreed within ±10%.

MgP_i protection against NBD-Cl reaction is presented in Fig. 2.6. It is evident that P_i protected well against NBD-Cl inhibition of ATPase activity in wild type and αG351Q mutant but did not protect at all against inactivation in αS347Q or αS347A mutants.

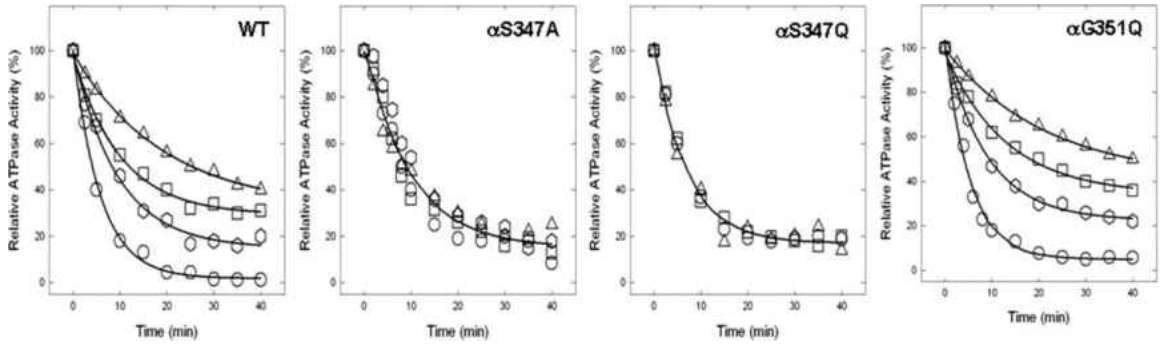

FIGURE 2.6. **Protection by Pi of ATPase activity in wild type (WT) and mutant membranes from inactivation by NBD-Cl.** The membranes were preincubated with MgPi at 0, 2.5, 5, or 10 mM concentration as shown, for 60 min at room temperature. Then NBD-Cl (150 μM) was added, and aliquots were withdrawn for assay at time intervals as shown. ATPase activity remaining is plotted against time of incubation with NBD-Cl. ○, no Pi added; ⬡, 2.5 mM Pi; □, 5 mM Pi; Δ, 10 mM Pi. Each data point represents the average of four different experiments using two independent membrane preparations of each mutant.

Inhibition of ATPase Activity by Fluoroaluminate, Fluoroscandium, and Azide—We next examined the effects of transition state and ground state analogs. Fig. 2.7 (*A* and *B*) show inhibition of wild type and mutant enzymes by MgADP-fluoroaluminate and MgADP-fluoroscandium, respectively. Wild type and αG351Q were completely inhibited. αS347A showed only ~25% inhibition. In contrast, the mutant αS347Q was remarkably resistant to inhibition. Azide is also a potent inhibitor of ATPase in ATP synthase. Fig. 2.7*C* shows that although wild type is strongly inhibited by azide, the mutants showed varied resistance with ~70% inhibition in αG351Q and only ~20–25% inhibition in αS347Q and αS347A mutants.

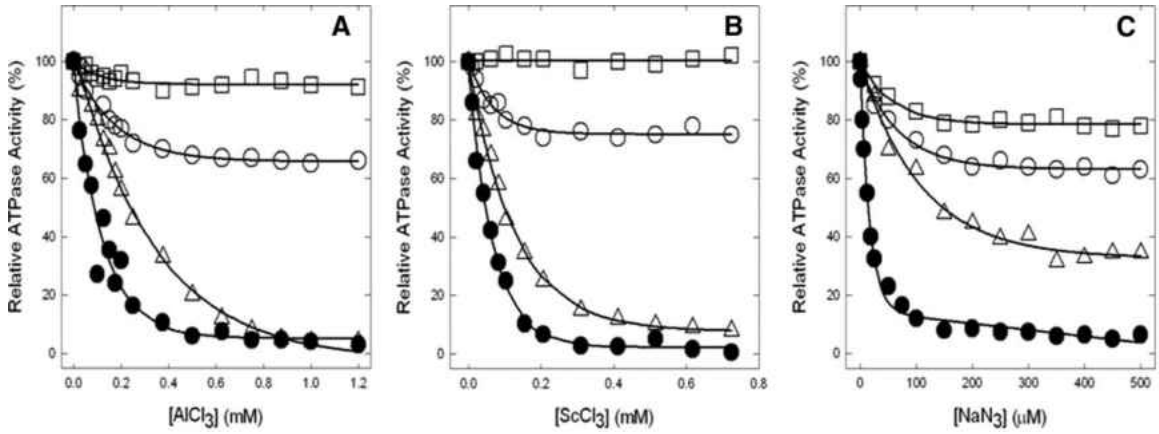

FIGURE 2.7. **Inhibition of membrane ATPase activity from mutant and wild type ATP synthase enzymes by fluoroaluminate, fluoroscandium, and azide.** The membranes were preincubated for 60 min at room temperature with 1 mM MgADP, 10 mM NaF, and the indicated concentrations of AlCl3 (*A*) or ScCl3 (*B*). Then aliquots were added to 1 ml of assay buffer, and ATPase activity was determined. Sodium azide was added directly to the membranes and incubated for 30 min before assay (*C*), for details see "Materials and Methods." ●, wild type; ○, αS347A; □, αS347Q; Δ, αG351Q. All of the data points are the means of at least quadruplicate experiments. The variation was ±10% between different experiments.

Inhibition of ATPase Activity by DCCD—Fig. 2.8 shows the wild type and αS347Q, αS347A, and αG351Q mutant enzymes inactivated by DCCD. Although wild type is completely inhibited by 200 μM DCCD after16 h of incubation at room

temperature, mutants show varied degrees of inhibition. αG351Q is inhibited about 10%, αS347A is inhibited only ~30%, and αS347Q is not inhibited at all. In a similar series of experiments, carried out with the same range of DCCD concentrations and reaction conditions, but for only 2- or 5-h incubations, we found that wild type still became fully inhibited, αG351Q and αS347Q both showed zero inhibition, and αS347A was inhibited maximally by 6% (2 h) and 15% (5 h).

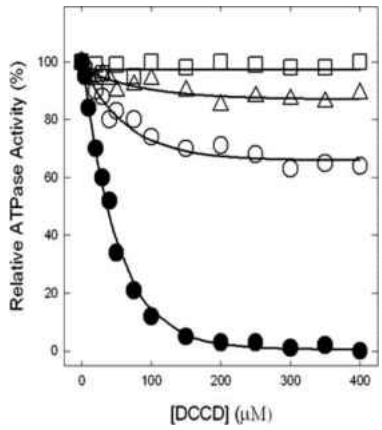

FIGURE 2.8. **Inhibition of membrane ATPase activity from mutant and wild type ATP synthase enzymes by DCCD.** The membranes were preincubated for 16 h at room temperature with varied concentrations of DCCD indicated in the figure. Then 1 ml of ATPase assay buffer was added to determine the activity. ●, wild type; ○, αS347A; □, αS347Q; Δ, αG351Q. All of the data points are means of at least quadruplicate experiments. The variation was ±10% between different experiments.

Discussion

The goal of this study was to examine the functional role(s) of residue αSer-347 and αGly-351 of *E. coli* ATP synthase. These residues are part of the strongly conserved α-subunit VISIT-DG sequence. The VISIT-DG sequence residues are located in close proximity to the α/β interface flanking the P_i-binding pocket (Fig. 2.1*B*). X-ray crystal structures of the AlF_3-inhibited enzyme (22) as well as the AlF_4^- inhibited enzyme (which also contained SO_4^{2-} in a second catalytic site) (23) show that the side chain of residue

αSer-347 is very close to these bound P_i analogs (Fig. 2.1) and that αGly-351 is also close. P_i binding is a primary step in ATP synthesis by ATP synthase, thus exploring the molecular basis of P_i binding is an important way to examine and understand the functional role of residues in the catalytic site.

Earlier studies established that mutagenesis combined with the use of the P_i protection assay against NBD-Cl inhibition, as well as the use of inhibitory analogs, enabled characterization of functional role(s) of residues suspected to be involved in P_i binding (24–30). From analysis of six such catalytic site residues, we determined that four residues, namely, αArg-376, βArg-182, βArg-246, and βLys-155, are critical for P_i binding and form a triangular subdomain within the catalytic site (24–30) (Fig. 2.1*B*). We also established that introduction of a negative or positive charge in this location resulted in drastic modulation of P_i binding (25, 26, 30), indicating that negative charge within the triangular subdomain was an important determinant of P_i binding. Here we used the same approaches to study residues αSer-347 and αGly-351.

We introduced the mutations αS347Q, αS347A, and αG351Q, none of which affected assembly nor structural integrity of the membrane ATP synthase. Membranes showed similar content of F_1-α and β subunits as compared with wild type. Both αS347Q or αG351Q mutations had severely inhibitory effects on oxidative phosphorylation as judged by growth on succinate or limiting glucose medium, and both strongly inhibited ATPase activity. On the other hand the αS347A mutation showed small residual oxidative phosphorylation and ATPase activity (Table 2.1). The results with the αS347Q and αS347A mutants showed that they abolished P_i binding (Fig. 2.6).

Although based on Table 2.1 data for αS347A mutant, it can be argued that there could be a small amount of P_i binding in cells but not significant enough to be measurable in the P_i binding assay of membranes (Fig. 2.6). Fluoroaluminate and fluoroscandium in combination with MgADP potently inhibit wild type *E. coli* ATP synthase (24–27, 30, 47, 48), and both are believed to mimic the chemical transition state. Transition state-like structures involving bound MgADP- AlF_4^- complex have been seen in catalytic sites in ATP synthase by x-ray crystallography (23). It was evident that the αS347Q mutant strongly destabilized the transition state (Fig. 2.7, *A* and *B*), because no inhibition by MgADP-fluoroaluminate or MgADP-fluoroscandium was apparent. Clearly, therefore, residue αSer-347 is involved directly and to an important degree in catalysis and may be added as a fifth member of the group of P_i-binding residues that make up the triangular P_i-binding pocket. αS347A mutant did show some residual inhibition (~25%) with both MgADP-fluoroaluminate and MgADP-fluoroscandium, which is in agreement with the partial oxidative phosphorylation and ATPase activity found in this mutant. In contrast, the αG351Q mutation did not prevent P_i binding (Fig. 2.6) and had lesser effects in destabilizing the transition state as judged by fluoroaluminate and fluoroscandium inhibition of ATPase (Fig. 2.7, *A* and *B*). Its effects on catalysis are therefore more indirect.

All of the mutations affected the degree of inhibition by azide, with αS347Q reducing it substantially (by ~80%), αS347A reducing it substantially (~75%), and αG351Q reducing it by ~30% (Fig. 2.7*C*). A recent x-ray crystallography study (49) showed that azide inhibits ATP synthase by forming a tightly binding MgADP-azide complex in βDP catalytic sites, which resembles that formed by MgADP-beryllium

fluoride and may therefore be considered an analog of the MgATP ground state. In the MgADP-azide complex, azide occupies a position equivalent to that of the γ-phosphate of MgATP. Thus mutants also had effects on substrate binding by virtue of an effect at the γ-phosphate position.

DCCD inhibits wild type *E. coli* F_1 by reacting with residue βGlu-192 (50) and/or *c*Asp-61 (51), with the latter predominating at lower DCCD concentration and/or shorter incubation time. As expected, wild type ATP synthase was inhibited almost 100%. αS347Q mutant was not inhibited at all, αG351Q was inhibited to ~10%, and mutant αS347A is inhibited ~30% (Fig. 2.8). Notably, at shorter incubation times, αS347A showed even less inhibition (see "Results"). The data therefore indicate that in the αS347A mutant, ATPase activity on F_1 is only partly coupled to proton translocation in F_o, which explains why αS347A mutant retains some growth on succinate and in limiting glucose (Table 2.1). It is interesting to note here that P_i binding and release events have been shown to be directly linked to rotation of the central stalk in single molecule experiments (52). Perturbation of the P_i-binding site might well be anticipated to perturb the integrity of the link between P_i binding and rotation and be manifested as uncoupling. The overall data on αS347A mutant strongly suggests that the Ser-OH group is needed for transition state stabilization and P_i binding.

The availability of x-ray structures allows one to discuss in detail the roles of residues αSer-347 and αGly-351. αSer-347 is positioned close to bound AlF_4^- in catalytic sites (Fig. 2.1*B*) (23). The Ser-OH lies 5.0 Å from the F1 and F3 atoms in AlF_4^- and thus may contribute to transition state stabilization by direct interaction.

It may be remarked that a similar conclusion was reached regarding the Ser-OH of the highly conserved LSGGQ ABC signature sequence in P-glycoprotein (17). Considering how P_i binding is affected, αSer-347-OH lies 6.1 Å from atom O_2 in SO_4^{2-} (23) and 4.6 Å from F1 of AlF_3 in the respective catalytic sites (22). Thus some direct interaction may be operative. However, more important than the above may be the fact that the Ser-OH lies 3.2 Å from the NH_2 of βArg-246 (in the AlF_4^- site) and 3.0 and 4.1 Å, respectively from NH_2 and NH1 of βArg-246 in the AlF_3-occupied site. βArg-246 is strongly conserved and critical for P_i binding and transition state stabilization (24). Further, the carbonyl-O of αSer-347 lies 3.2 Å from NH_2 of βArg-182, another P_i-binding residue. The likely H-bond interaction between αSer-347 and βArg-246 (and βArg-182) suggests these residues act together to support P_i binding and transition state stabilization. αGly-351 is located at a distance of 7.7 Å from AlF_4^- and 8.7 Å from SO_4^{2-}. A more indirect role in catalysis is therefore indicated, likely predominantly structural in nature.

In summary, both αSer-347 and αGly-351 of the conserved VISIT-DG sequence in ATP synthase α-subunit are required for catalysis. αSer-347 plays the more important role and is required for P_i binding and transition state stabilization.

Acknowledgments

We are thankful to Dr. Wayne Frasch (School of life Sciences, Arizona State University, Tempe, AZ) for helpful discussions. We are also grateful to Dr. Scott Champney (Department of Biochemistry and Molecular Biology, East Tennessee State University) for allowing us to use their ultracentrifuge and the Department of Biological Sciences at East Tennessee State University for providing additional funding for the purchase of a

new French press and ultracentrifuge.

Footnotes

* This work was partly supported by East Tennessee State University Major Research Development Committee Grant 0061 (to Z. A.) and Student-Faculty Collaborative Research Grants through Honors College, East Tennessee State University.

[1] To whom correspondence should be addressed: Dept. of Biological Sciences, Box 70703, East Tennessee State University, Johnson City, TN 37614. Tel.: 423-439-6931; Fax: 423-439-5958; E-mail: ahmadz@etsu.edu.

[2] The abbreviations used are: AMP-PNP, 5′adenylyl-β, γ-imidodiphosphate; NBD-Cl, 7-chloro-4-nitrobenzo-2-oxa-1, 3-diazole; DTT, dithiothreitol; TES, 2-{[2-hydroxy-1,1-bis(hydroxymethyl)ethyl]amino}ethanesulfonic acid; DCCD, dicyclohexylcarbodiimide.

[3] *E. coli* residue numbers are used throughout.

References

1. Senior, A. E. (1988) *Physiol. Rev.* **68,** 177-231
2. Fillingame, R. H. (1990) *The Bacteria*, Vol. XII, pp. 345-391, Academic Press, Orlando, FL
3. Karrasch, S., and Walker, J. E. (1999) *J. Mol. Biol.* **290,** 379-384
4. Devenish, R. J., Prescott, M., Roucou, X., and Nagley, P. (2000) *Biochim. Biophys. Acta* **1458,** 428-442

5. Abrahams, J. P., Leslie, A. G. W., Lutter, R., and Walker, J. E. (1994) *Nature* **370,** 621-628
6. Diez, M., Zimmerman, B., Börsch, M., König, M., Schweinberger, E., Steigmiller, S., Reuter, R., Felekyan, S., Kudryavtsev, V., Seidel, C. A. M., and Gräber, P. (2004) *Nat. Struct. Mol. Biol*. **11,** 135-141
7. Itoh, H., Takahashi, A., Adachi, K., Noji, H., Yasuda, R., Yoshida, M., and Kinosita, K. (2004) *Nature* **427,** 465-468
8. Noji, H., and Yoshida, M. (2001) *J. Biol. Chem*. **276,** 1665-1668
9. Weber, J., and Senior, A. E. (2003) *FEBS Lett*. **545,** 61-70
10. Pedersen, P. L. (2005) *J. Bioenerg. Biomembr*. **37,** 349-357
11. Weber, J. (2007) *Trends. Biochem. Sci.* **32,** 53-56
12. Frasch, W. D. (2000) *Biochim. Biophys. Acta* **1458,** 310-325
13. Ren, H., and Allison, W. S. (2000) *Biochim. Biophys. Acta* **1458,** 221-233
14. Boyer, P. D. (1989) *FASEB J.* **3,** 2164-2178
15. Al-Shawi, M. K., and Senior, A. E. (1992) *Biochemistry* **31,** 886-891
16. Al-Shawi, M. K., Ketchum, C. J., and Nakamoto, R. K. (1997) *Biochemistry* **36,** 12961-12969
17. Tombline, G., Bartholomew, L., Gimi, K., Tyndall, G. A., and Senior, A. E. (2004) *J. Biol. Chem.* **279,** 5363-5373
18. Löbau, S., Weber, J., and Senior, A. E. (1998) *Biochemistry.* **37,** 10846-10853
19. Weber, J., and Senior, A. E. (1995) *J. Biol. Chem*. **270,** 12653-12658
20. Perez, J. A., Greenfield, A. J., Sutton, R., and Ferguson, S. J. (1986) *FEBS Lett.* **198,** 113-118

21. Orriss, G. L., Leslie, A. G. W., Braig, K., and Walker, J. E. (1998) *Structure* **6,** 831-837

22. Braig, K., Menz, R. I., Montgomery, M. G., Leslie, A. G. W., and Walker, J. E. (2000) *Structure* **8,** 567-573

23. Menz, R. I., Walker, J. E., and Leslie, A. G. W. (2001) *Cell* **106,** 331-341

24. Ahmad, Z., and Senior, A. E. (2004) *J. Biol. Chem*. **279,** 31505-31513

25. Ahmad, Z., and Senior, A. E. (2004) *J. Biol. Chem*. **279,** 46057-46064

26. Ahmad, Z., and Senior, A. E. (2005) *J. Biol. Chem*. **280,** 27981-27989

27. Ahmad, Z., and Senior, A. E. (2005) *FEBS Lett.* **579,** 523-528

28. Ahmad, Z., and Senior, A. E. (2005) *J. Bioenerg. Biomembr*. **37,** 437-440

29. Ahmad, Z., and Senior, A. E. (2006) *FEBS Lett*. **580,** 517-520

30. Brudecki, L. E., Grindstaff, J. J., and Ahmad, Z. (2008) *Arch. Biochem. Biophys.* **471,** 168-175

31. Penefsky, H. S. (2005) *FEBS Lett*. **579,** 2250-2252

32. Senior, A. E., Nadanaciva, S., and Weber, J. (2002) *Biochim. Biophys. Acta* **1553,** 188-211

33. Chen, C., Saxena, A. K., Simcoke, W. N., Garboczi, D. N., Pedersen, P. L., and Ko, Y. H. (2006) *J. Biol. Chem.* **281,** 13777-13783

34. Ketchum, C. J., Al-Shawi, M. K., and Nakamoto, R. K. (1998) *Biochem. J.* **330,** 707-712

35. Vandeyar, M., Weiner, M., Hutton, C., and Batt, C. (1988) *Gene* (Amst.) **65,** 129-133

36. Weber, J., Wilke-Mounts, S., Lee, R. S. F., Grell, E., and Senior, A. E. (1993) *J. Biol. Chem.* **268,** 20126-20133

37. Weber, J., Hammond, S. T., Wilke-Mounts, S., and Senior, A. E. (1998) *Biochemistry* **37,** 608-614

38. Klionsky, D. J., Brusilow, W. S. A., and Simoni, R. D. (1984) *J. Bacteriol*. **160,** 1055-1060

39. Senior, A. E., Langman, L., Cox, G. B., and Gibson, F. (1983) *Biochem. J*. **210,** 395-403

40. Senior, A. E., Latchney, L. R., Ferguson, A. M., and Wise, J. G. (1984) *Arch. Biochem. Biophys.* **228,** 49-53

41. Taussky, H. H., and Shorr, E. (1953) *J. Biol. Chem*. **202,** 675-685

42. Laemmli, U. K. (1970) *Nature* **227,** 680-685

43. Rao, R., Perlin, D. S., and Senior, A. E. (1987) *Arch. Biochem. Biophys.* **255,** 309-315

44. Weber, J., Wilke-Mounts, S., and Senior, A. E. (1994) *J. Biol. Chem*. **269,** 20462-20467

45. Ferguson, S. J., Lloyd, W. J., Lyons, M. H., and Radda, G. K. (1975) *Eur. J. Biochem.* **54,** 117-126

46. Ferguson, S. J., Lloyd, W. J., and Radda, G.K. (1975) *Eur. J. Biochem*. **54,** 127-133

47. Nadanaciva, S., Weber, J., and Senior, A. E. (2000) *Biochemistry* **39,** 9583-9590

48. Nadanaciva, S., Weber, J., and Senior, A. E. (1999) *J. Biol. Chem*. **274,** 7052-7058

49. Bowler, M. W., Montgomery, M. G., Leslie, A. G., and Walker, J. E. (2006) *Proc. Natl. Acad. Sci. U. S. A.* **103,** 8646-8649

50. Yoshida, M., Allison, W. S., Esch, F. S., and Futai, M. (1982) *J. Biol. Chem*. **257,** 10033-10037

51. Hermolin, J., and Fillingame, R. H. (1989) *J. Biol. Chem*. **264,** 3896-3908

52. Adachi, K., Oiwa, K., Nishizaka, T., Furuike, S., Noji, H., Itoh, H., Yoshida, M., and Kinosita, K. (2007) *Cell* **130,** 309-321

CHAPTER 3

MODULATION OF ALPHA-SUBUNIT VISIT-DG SEQUENCE RESIDUE THR-349 IN THE CATALYTIC SITES OF *ESCHERICHIA COLI* ATP SYNTHASE[*]

Laura E. Brudecki[‡1] and Zulfiqar Ahmad

[‡]Department of Biological Sciences, East Tennessee State University, Johnson City, Tennessee 37614

[1]To whom correspondence should be addressed: Dept. of Biological Sciences, Box 70703, East Tennessee State University, Johnson City, TN 37614. Tel.: 423-439-6931; Fax: 423-439-5958; E-mail: laurabrudecki@gmail.com.

Abstract

ATP synthase is responsible for the synthesis and hydrolysis of ATP, cellular energy. Much is known about the structure and function of ATP synthase from various organisms and tissues, but more knowledge needs to be obtained in order to modulate the enzyme for use in nanotechnology. In order to understand the catalytic mechanisms of ATP synthase, we must come to understand the role of residues within the P_i binding site. P_i binding is an essential part of ATP synthesis. Five residues within the catalytic site have previously been shown to bind P_i. Here we investigate the role of αThr-349 of the VISIT-DG sequence through mutagenic analysis. αT349A/D/R, αT349R/βR182A, and βR182A mutants were generated. Results from preliminary experiments suggest that αThr-349 may play a role in P_i binding, but further investigation is required.

Introduction

ATP synthase is an enzyme found in nearly every organism, ranging from bacteria to humans. ATP synthase is also the smallest known molecular motor. This enzyme is responsible for the majority of cell energy production through the synthesis of adenosine-5'-triphosphate (ATP) from adenosine-5'-diphosphate (ADP) and inorganic phosphate (P_i). The structure of this enzyme is similar in all organisms with some amino acid sequence residues being highly conserved throughout evolution (1-5). *E. coli* ATP synthase consists of eight subunits that are divided into two sectors. The water-soluble F_1 sector contains subunits α_3, β_3, δ, ε, and γ, while the membrane bound F_O sector houses a, b_2, and c_{10} subunits (1-8). F_1-ATPase has six nucleotide binding sites on the α/β hexamer; three are catalytic and three are non-catalytic (9). Each of these sites is located on the interface between α and β. ATP, ADP, and P_i bind at the βTP, βDP, and βE sites,

respectively.

Through mutagenic analysis, it is possible to characterize the function of individual amino acid residues, specifically within the α/β-catalytic sites. Eight residues in close proximity to the catalytic site have been studied, and it was found that βArg-246, αArg-376, βLys-155, βArg-182, and αSer-347 are responsible for binding P_i, a determining factor in the synthesis of ATP (3, 10-12); and βAsn-243, βPhe-291, and αGly-351 were found to be important for overall function but not in P_i binding (3, 13, 14)[1].

Alpha subunit VISIT-DG sequence residues are near to the phosphate-binding subdomain and may potentially be essential for P_i binding (3). αSer-347 of the VISIT-DG sequence was the fifth residue recently found to be important for P_i binding (3). Is αThr-349 involved in P_i binding or transition state? Is there a charge communication between the hydroxyl group of αThr-349 and its close neighbor βR182?

We modulated the size and charge of αThr-349 by mutating it to arginine, alanine, and aspartic acid. In order to test the hypotheses related to its involvement in Pi binding and structural support the following mutations were constructed: αT349A, αT349D, αT349R, βR182A, and αT349R/βR182A. We predict that αThr-349 has a similar function to that of αSer-347, that the mutations αT349A, αT349R, and αT349D will affect P_i binding and transition state, and that the mutation αT349R/βR182A will show a compensatory effect for the loss of βR182.

Materials and Methods

Construction of αThr-349 mutations in E. coli -- Site-directed mutagenesis was performed using a QuickChange Lightning Site-Directed Mutagenesis Kit from

Stratagene. Plasmid DNA was isolated from pSN6, a βY331W mutant from a pBWU13.4/DK8 strain, which has been used in previous studies from our lab. pSN6 is a plasmid containing the βY331W mutation from plasmid pSWM4 (15) introduced on a SacI-EagI fragment into pBWU13.4 (16), which expresses all the ATP synthase genes (3).This mutation was inserted into the wild-type strain for use in fluorescence studies and has not been shown to inhibit function of the enzyme (15). Use of this strain enables new mutants to be used in fluorescence studies as well as our work of interest.

The QuickChange Lightning Multi Site-Directed Mutagenesis Kit comes with a QuikChange Multi control template from the pBluescript II SK (-) which encodes for β-galactosidase by the *LacZ* gene. The use of the template along with the control primer mutates the template from having three early stop codons to a functional triple mutant for β-galactosidase (17, 18). If the *LacZ* gene is interrupted, the cell will no longer be able to synthesize galactosidase, an enzyme responsible for the breakdown of lactose, and no color change will occur in the presence of IPTG, the gene's inducer, and X-Gal, the substrate for the enzyme (17, 18). Hence, when the early stop codons are removed, the gene product will again be functional, and the presence of blue colonies will indicate that the mutagenesis was successful. Mutagenic oligonucleotides are shown in Table 3.1. Reaction mixes were transformed into XL10-Gold Ultracompetent Cells and plated on LB ampicillin agar plates as per kit. Colonies were picked from plates and grown in 10 ml LB ampicillin broth for ~8 hr at 250 rpm. Plasmid DNA was isolated using a Promega Wizard Plus SV MiniPrep Kit. Supernatant from the first pellet was saved for sample recovery. Mutant DNA was transformed into strain DK8 and sent for sequencing to test for any undesired changes and that the desired mutation was correct. Strain DK8

contains a deletion of ATP synthase genes for expression of the mutant enzymes (3).

TABLE 3.1 **Mutagenic oligonucleotides for constructing αT349 and βR182 mutants**

Strain	Mutation	Mutagenic Oligonucleotide	New Restriction Site
pLEB5	αT349R/βY331W	GTTCCGACCAACGTAATCTCCATT CGCGATGGTCAGATCT	NruI
pLEB10	αT349D/βY331W	GTTCCGACCAACGTAATCTC**A**ATT GACGATGGTCAGATCTTCCTGG	MfeI
pLEB13	αT349A/βY331W	GTTCCGACCAACGTAATC**T**ATAG CCGATGGTCAGATCTTCCTG	SfcI
pLEB14	βR182A/βY331W	GTTTGCGGGCGTAGGTGAAGCTA CTCGTGAGG	AluI
pLEB15	αT349R/βR182A/ βY331W	The oligonucleotide for pLEB14 was used on the pLEB5 plasmid	NruI and AluI

All mutants were expressed with the βY331W mutation also present. The underlined nucleotide bases introduce the new mutation, and bold letters signify a silent mutation. Mutations and silent mutations inserted new restriction sites; however, plasmids were sent directly for sequencing and were not screened using restriction digestion.

Newly developed mutants, αT349A, αT349D, αT349R, βR182A, and αT349R/βR182A, were assayed for growth and used in biochemical.

Growth in Limiting Glucose and on Succinate Medium--Modulation of these residues was undertaken using growth on limiting glucose and succinate media and through biochemical assays. Mutants were grown in limiting glucose media as in (19). Growth was measured by reading the OD_{595} every hour until the growth reached late log phase. Succinate minimal media plates were also streaked and grown overnight as in (3). Plates were left out at room temperature for further growth. Growth on succinate plates were given a rating of no growth (-), partial growth (++), and heavy growth (+++) for the next three days. Growth on succinate and limiting glucose were compared. Once growth assays are completed satisfactorily, bacterial membrane-bound F_1F_O preparations will be made for use in biochemical assays.

Preparation of E. coli membrane bound ATP synthase—Membrane-bound F_1F_O

ATP synthase was prepared as in (20). Membrane pellets were washed three times in buffer. The first wash is performed in buffer containing 50 mM TES, pH 7.0, 15% glycerol, 40 mM 6-aminohexanoic acid, 5 mM *p*-aminobenzamidine. The following two washes are performed in buffer containing 5 mM TES, pH 7.0, 15% glycerol, 40 mM 6-aminohexanoic acid, 5 mM *p*-aminobenzamidine, 0.5 mM dithiothreitol (DTT), and 0.5 mM EDTA. Pellets were finally resuspended in 50mM Tris-Sulfate, pH 8.0, and 2.5mM $MgSO_4$, and stored in -20°C.

Concentration of total protein was found using the method of Bradford (21). ATPase activity was measured in 1 ml of assay buffer containing 10 mM NaATP, 4 mM $MgCl_2$, 50 mM $TrisSO_4$, pH 8.5, at 37 °C. Addition on membranes began the reaction and the addition of SDS^2 to 3.3% final concentration stopped the reaction. P_i released was assayed as in (22). For wild type membranes (20–30 μg of protein), reaction times were 5–10 min. For mutant membranes (20–100 μg of protein), reaction times were 15–90 min. All of the reactions were shown to be linear with time and protein concentration.

NBD-Cl (7-chloro-4-nitrobenzo-2-oxa-1, 3-diazole) inhibition, extra pulse of NBD-Cl, reversibility of NBD-Cl inhibition by DTT, and protection from NBD-Cl inhibition by MgADP and MgPi assays were used to show if the mutant catalytic sites are still able to bind inhibitors and substrates and to what degree they favor binding.

Inhibition of ATP Synthase activity by NBD-Cl, Extra Pulse of NBD-Cl, and Reversal of NBD-Cl Inhibition by DTT —NBD-Cl was prepared as a stock solution in dimethyl sulfoxide and protected from light. The membranes (0.2–1 mg/ml) were reacted with NBD-Cl for 60 min in the dark at room temperature in 50 mM $TrisSO_4$, pH 8.0, 2.5 mM $MgSO_4$, and then 50-μl aliquots were transferred to 1 ml of ATPase assay buffer to

determine ATPase activity. For extra pulse of NBD-CL, the membranes were first reacted with NBD-Cl (150 μM) for 1 h at room temperature, and then reacted with an extra pulse of NBD-Cl (150 μM) for an additional hour at room temperature before ATPase assay. Control samples without NBD-Cl were incubated for the same times. For reversal of NBD-Cl inhibition by DTT, the membranes were first reacted with NBD-Cl (150 μm) for 1 h at room temperature, and then DTT (final = 4 mm) was added, and incubation continued for 1 h at room temperature before ATPase assay. Control samples without NBD-Cl and/or DTT were incubated for the same times.

Protection of ATP Synthase Activity from Inhibition by NBD-Cl with MgADP and MgP_i--Membranes were preincubated 60 min with protecting agent at room temperature before the addition of NBD-Cl. $MgSO_4$ was present, equimolar with ADP or P_i. ATPase activity was assayed after 0 min to 1 h incubation with NBD-Cl in 5 min increments. Control samples containing the ligand without added NBD-Cl were included. Neither P_i (up to 50 mM) nor MgADP (up to 10 mM) had any inhibitory effect alone.

TABLE 3.2 **Effects of αThr-349 and βArg-182 mutation on cell growth and ATPase activity**

Mutation[a]	**Growth on succinate**[b]	**Growth yield in limiting glucose**	**ATPase activity**[c]
		%	*μmol/min/mg*
Wild type	++++	100	7
Null	–	37	N/A
βY331W	++++	94	N/A
αT349R	++	49	.07
αT349D	++	61	.4
αT349A	++	55	2
βR182A	++	47	.01
αT349R/βR182A	+	48	0.2

[a]Wild type, pBWU13.4/DK8; Null, pUC118/DK8, αT349R/DK8, αT349D/DK8, and αT349A/DK8.

[b]Growth on succinate plates after 3 days estimated visibly. ++++, heavy growth; ++, partial growth; –, no growth.

[c]ATPase activity was measured at 37°C and expressed as μmol of ATP hydrolyzed/min/mg of total protein. Data represent the mean from four to six assays. Data were obtained from one growth experiment and one membrane preparation and should not be considered conclusive. N/A= not assayed.

Growth properties of mutant enzymes--Once mutagenesis was completed, growth was assayed in limiting glucose and on succinate plates. Growth on Succinate, a non-fermentable carbon source, reveals the level of oxidative phosphorylation that may be achieved for the mutant strains. All mutants had a loss of oxidative phosphorylation. With the exception of αT349D, all mutant growth in limiting glucose was reduced to that of the null (pUC118). As shown in Table 3.2, growth on succinate and limiting glucose seemed to correlate, but as mentioned in the table legend, these assays need to be

duplicated in order to be conclusive. ATPase activity levels were low for all strains. Wild-type ATPase activity is generally ~28 μmol/min/mg, as in (3), but is only 7 μmol/min/mg from this particular membrane preparation. Low ATPase activity can result from poorly purified membrane, exposure to ambient temperatures, loss of F_1 during membrane prepartion, or chemical contaminants (3). Table 3.2 shows that in comparison to wild-type, ATPase activity of αT349R was reduced 100-fold, αT349D 18-fold, αT349A 4-fold, βR182A 700-fold, and αT349R/βR182A 40-fold.

Inhibition of ATP Synthase activity by NBD-Cl, Extra Pulse of NBD-Cl, and Reversal of NBD-Cl Inhibition by DTT-- NBD-Cl inhibition was assayed for wild-type and all mutant membrane-bound F_1F_O ATP synthase. Purified F_1 was not used in any of the following biochemical assays, as it has been shown that purified F_1 and membrane-bound F_1F_O behave similarly (3). In Figure 3.1, wild-type is shown to be completely inhibitied by NBD-Cl. X-ray crystallographic structures have shown that NBD-Cl binds to βY311 in bovine ATP synthase (βY297 in *E. coli*) by a covalent bond which results in loss of function (3, 23). αT349A behaved as wild-type and was potently inhibited with no residual activity. αT349R and αT349D were inhibited ~80-90%, maintaining ~20-10% residual activity. βR182A and αT349R/βR182A were inhibited only by ~50%.

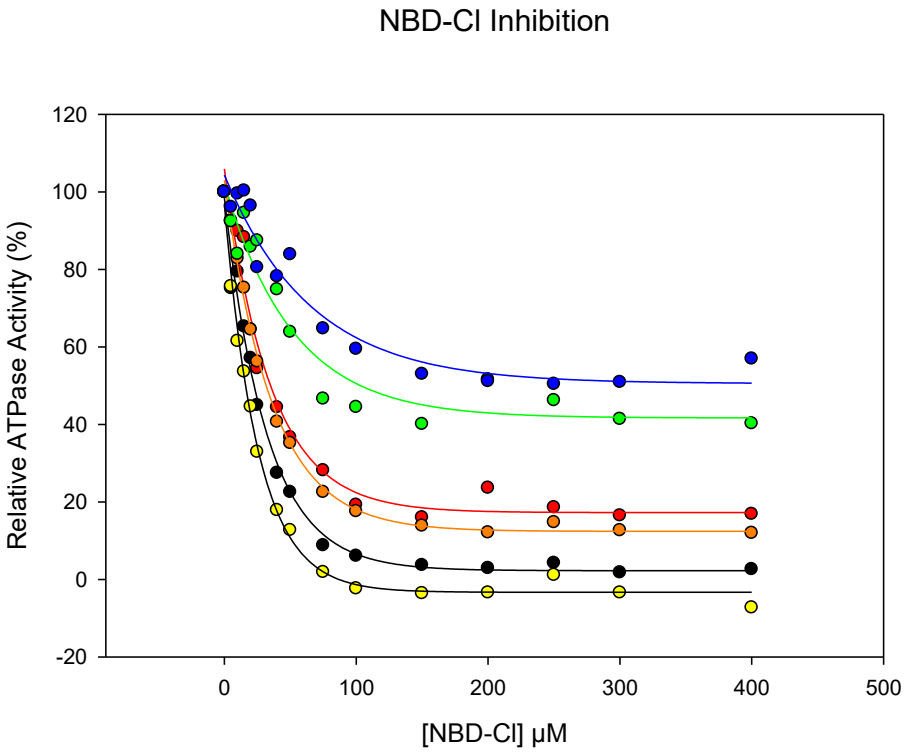

Figure 3.1. **Inhibition of ATPase activity by NBD-Cl.** The membranes were preincubated for 60 min at room temperature with varied concentrations of NBD-Cl, and then aliquots were added to 1 ml of assay buffer and ATPase activity was determined. The details are given under "Materials and Methods." Black, wild type; red, αT349R; orange, αT349D; yellow, αT349A; green, βR182A; blue, αT349R/βR182A. Each data point represents an average of at least two experiments.

In previous studies, mutant enzymes were not always completely inhibited by NBD-Cl. For this reason, we performed the NBD-Cl inhibition assay and after the initial one hour incubation with inhibitor, we applied an extra-pulse of 150 µM NBD-Cl followed by an additional hour of incubation (Figure 3.2). It was shown that little to no further inhibition is achieved, which confirms that some mutants do retain residual activity when reacted with NDB-Cl.

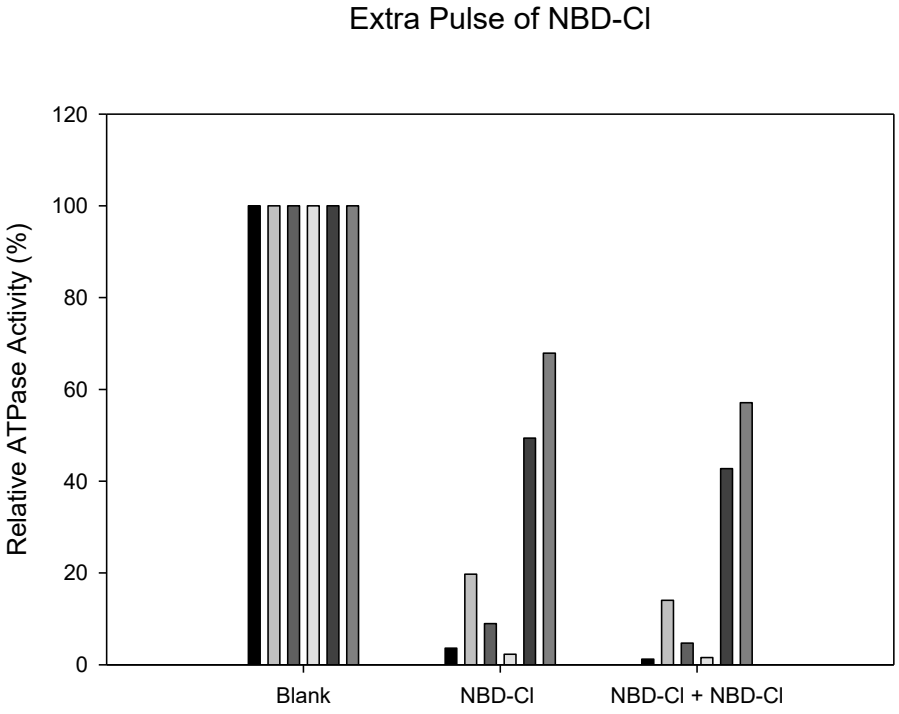

Figure 3.2. **Inhibition by an Extra Pulse of NBD-Cl.** Membrane ATP synthase was inhibited with 150 μM NBD-Cl for 60 min under conditions as described in Fig. 3.1. Then a further pulse of 150 μM NBD-Cl was added, and incubation continued for 1 h before assay. Each set of bars represents wild type, αT349R, αT349D, αT349A, βR182A, and αT349R/βR182A from *left* to *right*.

The NBD-O-Tyrosyl-297 covalent bond can be reversed through reaction with dithiothreitol (DTT) (23-25). Thus, reversal of NBD-Cl inhibition by DTT confirms that the NBD-Cl reacted in the βE catalytic site with Tyr-297 (3, 23-25). Figure 3.3 shows that reversal of inhibition was obtained in wild-type and mutant enzymes, confirming the reaction of NBD-Cl and βTry297. The absolute residual ATPase activity values are as follows: wild type, 6.47, 4.40, 6.54; αT349R, 0.07, 0.06, 0.07; αT349D, 0.55, 0.42, 0.55; αT349A, 2.40, 1.70, 2.27; βR182A, 0.01, 0.01, .001; and αT349R/βR182A, 0.02, 0.01, 0.02.

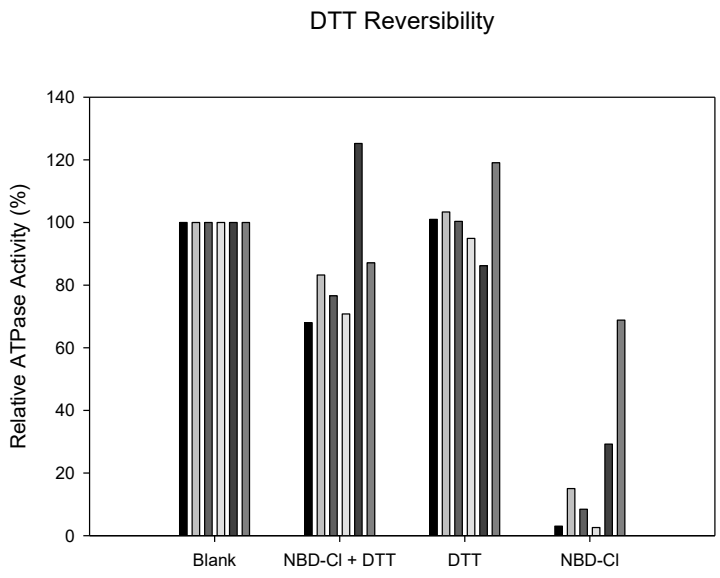

Figure 3.3. **Reversal of NBD-Cl effects by DTT.** Membrane ATP synthase was incubated with or without 150 μM NBD-Cl for 60 min under conditions as described for Fig. 3.1. In parallel samples, 4 mM DTT was then added, and incubation continued for further 60 min before assay. Each set of bars represents wild type, αT349R, αT349D, αT349A, βR182A, and αT349R/βR182A from *left* to *right*.

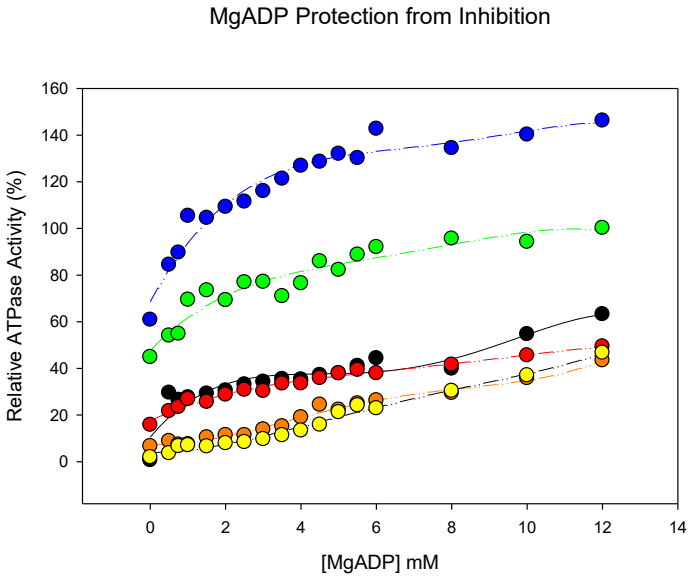

FIGURE 3.4. **Protection by MgADP against NBD-Cl inhibition.** Wild type and mutant membranes were preincubated for 1 h at room temperature with varied concentrations of MgADP as shown, then 150 μM NBD-Cl was added, and incubation continued at room temperature in the dark for 1 h. The aliquots were then assayed for ATPase activity. Black, wild type; red, αT349R; orange, αT349D; yellow, αT349A; green, βR182A; blue, αT349R/βR182A. The results are the means of at least two experiments.

Protection of ATP Synthase Activity from Inhibition by NBD-Cl with MgADP and MgP_i--MgADP (Fig. 3.4) and MgP_i (Fig. 3.5A, B, C, D, E, and F) were used to protect ATP synthase from NBD-Cl inhibition. In Figure 3.4, βR182A and αT349R/βR182A show considerable protection, while wild-type and other mutants only show partial protection.

There appears to be some P_i protection in the αT349A mutant (Fig. 3.5D) but not in the αT349R (Fig. 3.5B) and αT349D mutant (Fig. 3.5C). αT349A was inhibited to completion in the NBD-Cl assays (Fig. 3.1), but here retains some residual activity when treated with MgP_i (Fig. 3.5D). Mutants αT349R and αT349D are inhibited as in Figure 3.1 which shows that MgP_i treatment had no bearing on the degree of inhibition(Fig. 3.5B and C). Data are inconclusive with the βR182A (Fig. 3.5E) and αT349R/βR182A mutants (Fig. 3.5F). Aside from WT and pLEB13, which were both repeated once, the P_i assays were only completed one time. Therefore, Figure 3.5A, B, C, D, E, and F are results from preliminary experiments and the assays need to be repeated to confirm resolution of the data points.

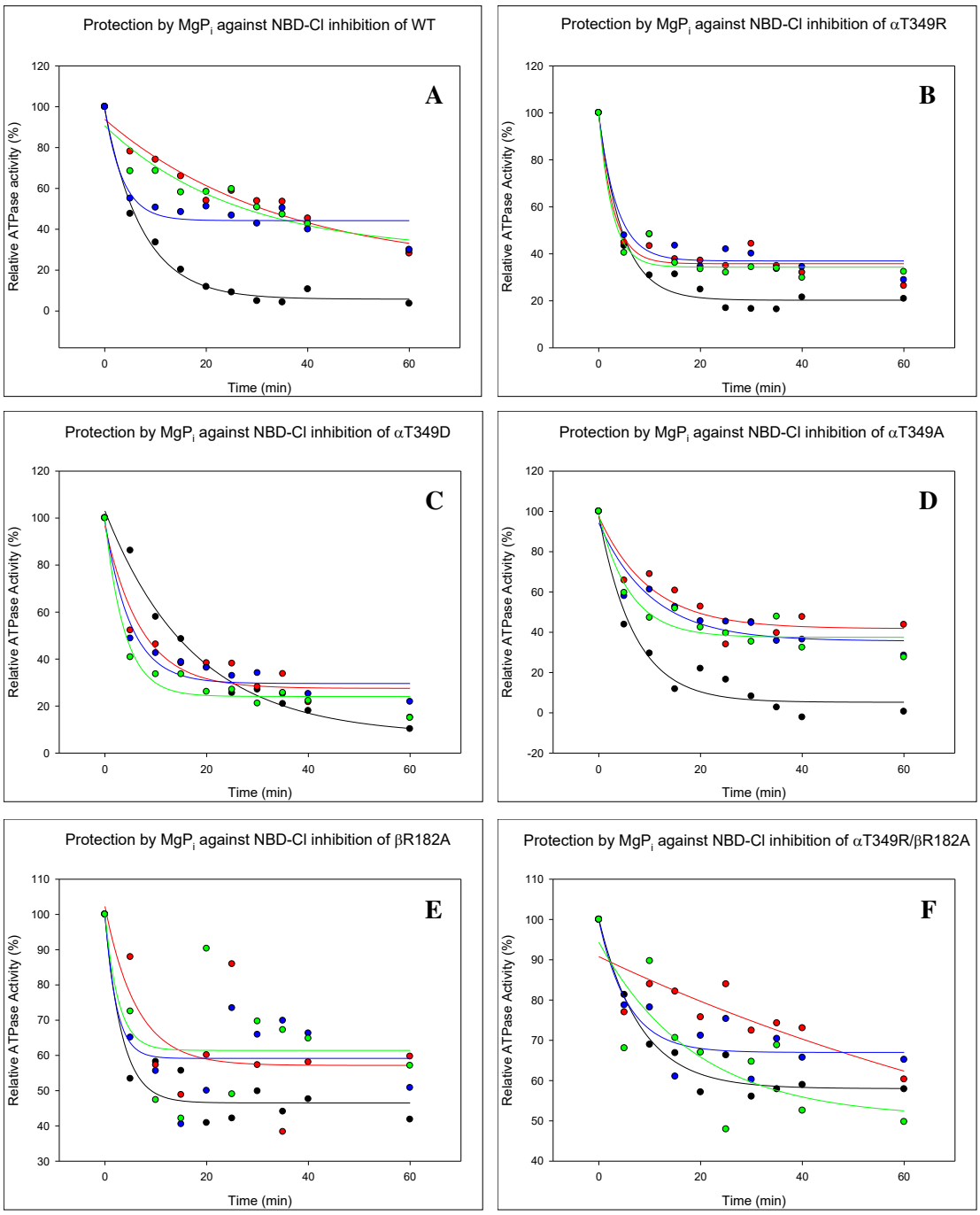

FIGURE 3.5. **Protection by MgP_i against NBD-Cl inhibition.** The membranes were preincubated with MgPi at 0, 2.5, 5, or 10 mM concentration as shown, for 60 min at room temperature. Then NBD-Cl (150 μM) was added, and aliquots were withdrawn for assay at time intervals as shown. ATPase activity remaining is plotted against time of incubation with NBD-Cl. black, no P_i added; red, 2.5 mM P_i; green, 5 mM P_i; blue, 10 mM P_i. A, WT; B, αT349R; C, αT349D; D, αT349A; E, βR182A; F, αT349R/βR182A. Each data point represents one experiment.

Sodium azide, fluoroaluminate, fluoroscandium, and DCCD assays have not yet been performed. In order to assess effects of mutations on transition state and coupling, these assays must be completed.

Discussion

Due to the highly conserved nature of ATP synthase α subunit VISIT residues and their close proximity to the P_i binding subdomain, VISIT sequence residues are of interest when characterizing phosphate binding residues in ATP synthase. Previously it was shown that αSer-347 is important for P_i binding, and that the –OH side chain of serine is required for transition state stabilization (3). The current work investigated the role of αThr-349 through the introduction of mutations αT349R, αT349D, αT349A, βR182A, and αT349R/βR182A.

Mutant enzymes showed a loss of oxidative phosphorylation as well as a decrease in ATPase activity compared to that of wild-type (Table 3.2). Certainty as to whether loss of function was due to mutation or structural integrity of the mutant enzymes is not clear.

NBD-Cl was able to bind the βE site of each mutant generated as shown by the DTT reversibility assay (Fig. 3.3). However, maximal NBD-Cl inhibition was not reached in all mutants: βR182A and αT349R/βR182A retained ~50% residual activity; αT349A behaved as wild-type and was potently inhibited with no residual activity; αT349R and αT349D were inhibited ~80-90%, and maintained ~20-10% residual activity.

Through the MgP_i assays, we found that mutants αT349R and αT349D appear not to be protected from NBD-Cl inhibition due to loss of P_i binding, but αT349A appears to

have afforded some protection against NBD-Cl inhibition (Fig. 3.5 B, C, and D). These results imply that the size and charge may be important for αT349 to bind P_i and that the –OH side chain may not play a role in direct P_i binding. However, due to the preliminary nature of these results and the absence of transition state assays, we are unable to make any definite conclusions as to the role of αT349 in direct or indirect P_i binding at this time. Mutations do seem to have some effect on function, but further investigation is required in order to identify the specific effects.

Additional work needed to characterize the role of αThr-349 and its relationship with βR182 entails completing fluoroaluminate, fluoroscandium, and sodium azide assays. Inhibition by DCCD should be analyzed. In order to characterize the effect mutations have on folding, fluorescence studies could be performed with the newly generated mutants as they all contain the βY331W mutation.

Acknowledgments

We would like to thank Nathan Weber and Dr. Tom Jones (Department of Biological Sciences, East Tennessee State University) for their financial and technical support in sequencing analysis. We are also thankful to Dr. Karl Joplin (Department of Biological Sciences, East Tennessee State University) for helpful discussions.

Footnotes

[1]To whom correspondence should be addressed: Dept. of Biological Sciences, Box 70703, East Tennessee State University, Johnson City, TN 37614. Tel.: 423-439-1000; Fax: 423-439-5958; E-mail: laurabrudecki@gmail.com.

[2]The abbreviations used are: SDS, sodium dodecyl sulfate; NBD-Cl, 7-chloro-4-nitrobenzo-2-oxa-1, 3-diazole; TES, 2-{[2-hydroxy-1,1-

bis(hydroxymethyl)ethyl]amino}ethanesulfonic acid; DTT, dithiothreitol; EDTA, 2,2',2",2"'-(Ethane-1,2-diyldinitrilo)tetraacetic acid; DCCD, dicyclohexylcarbodiimide, [3]*E. coli* residue numbers are used throughout.

* This work was partially supported by NIH Grant GM085771 to ZA; Student-Faculty Collaborative Research Grants through Honors College, ETSU; and the Department of Biological Sciences at East Tennessee State University.

References

1. Devenish, R. J., Prescott, M., Roucou, X., and Nagley, P. (2000) *Biochim Biophys Acta* **1458,** 428-442
2. Karrasch, S., and Walker, J. E. (1999) *J. Mol. Biol.* **290,** 379-384
3. Li, W., Brudecki, L. E., Senior, A. E., and Ahmad, Z. (2009) *J. Biol. Chem.* **284,** 10747-10754
4. Senior, A. E. (1988) *Physiol. Rev.* **68,** 177-231
5. Senior, A. E., Nadanaciva, S., and Weber, J. (2002) *Biochim. Biophys. Acta.* **1553,** 188-211
6. Boyer, P. D. (1997) *Annu. Rev. Biochem.* **66,** 717-749
7. Hong, S., and Pedersen, P. L. (2008) *Microbiol. Mol. Biol. Rev.* **72,** 590-641
8. Nakamoto, R. K., Baylis Scanlon, J. A., Al-Shawi, M. K. (2008) *Arch Biochem Biophys.* **476,** 43-50
9. Bald, D., Amano, T., Muneyuki, E., Pitard, B., Rigaud, J.-L., Kruip, J., Hisabori, T., Yoshidai, M., and Shibata, M. (1998) *J. Biol. Chem.* **273,** 865-870
10. Ahmad, Z., and Senior, A. E. (2004) *J. Biol. Chem.* **279,** 31505-31513
11. Ahmad, Z., and Senior, A. E. (2005) *FEBS Lett.* **579,** 523-528
12. Ahmad, Z., and Senior, A. E. (2006) *FEBS Lett.* **580,** 517-520
13. Ahmad, Z., and Senior, A. E. (2004) *J. Biol. Chem.* **279,** 46057-46064
14. Brudecki, L. E., Grindstaff, J. J., and Ahmad, Z. (2008) *Arch. Biochem. Biophys.* **471,** 168-175
15. Weber, J., Wilke-Mounts, S., Lee, R. S. F., Grell, E., and Senior, A. E. (1993) *J. Biol. Chem.* **268,** 20126-20133

16. Ketchum, C. J., Al-Shawi, M. K., and Nakamoto, R. K. (1998) *Biochem. J.* **330,** 707-712
17. Davies, J., and Jacob, F. (1968) *J. Mol. Biol.* **36,** 413-417
18. Agilent Technologies. QuikChange Lightning Multi Site-Directed Mutagenesis Kit Instruction Manual Catalog # 210513 and #210515 Revision B. Accessed Sep., 2010. http://www.genomics.agilent.com/files/Manual/210513.pdf
19. Senior, A. E., Latchney, L. R., Ferguson, A. M., and Wise, J. G. (1984) *Arch. Biochem. Biophys.* **228,** 49-53
20. Senior, A. E., Langman, L., Cox, G. B., and Gibson, F. (1983) *Biochem. J.* **210,** 395-403
21. Bradford, M. M. (1976) *Anal. Biochem.* **72,** 248-254
22. Taussky, H. H., and Shorr, E. (1953) *J. Biol. Chem.* **202,** 675–685
23. Orriss, G. L., Leslie, A. G. W., Braig, K., and Walker, J E. (1998) *Structure* **6,** 831–837
24. Ferguson, S. J., Lloyd, W. J., Lyons, M. H., and Radda, G. K. (1975) *Eur. J. Biochem.* **54,** 117-126
25. Ferguson, S. J., Lloyd, W. J., and Radda, G. K. (1975) *Eur. J. Biochem*. **54,** 127-133

CHAPTER 4

CONCLUSIONS AND DIRECTIONS FOR FUTURE WORK

Conclusions

The ATP synthase α subunit VISIT-DG sequence residues seem to play an important role in structure and/or function of the enzyme because of their highly conserved nature and close proximity to the catalytic site. αSer-347 of the VISIT-DG sequence has been shown to be required for P_i binding. This provides rationale for investigating the role of the other VISIT-DG residues.

The goal of this work was to understand which amino acid residues in and around the catalytic site are responsible for binding P_i. We established that αSer-347 of the VISIT-DG residue sequence is required for P_i binding, and that αGly-351 is not required for binding P_i but is important for function of the enzyme. Preliminary experiments for αThr-349 provide adequate reason to presume that this residue may also be required for P_i binding, but further investigation is required.

In order to use ATP synthase as a base model for nanomotor development, we must understand how the catalytic site can be modulated for improved catalytic function. Although solid conclusions may not be drawn from preliminary experiments on αThr-349 and its interactions with βArg-182, data suggest that loss of βArg-182 cannot be compensated for by insertion of arginine in place of αThr-349. If the mutation was able to compensate for the loss of the known P_i binding βArg-182 residue, we would expect behavior in biochemical assays to be similar to wild type. However, this is not observed.

Prior to this work, we were aware of four amino acid residues, βArg-246, αArg-376, βLys-155, and βArg-182, required for phosphate binding in the catalytic sites of *E.*

coli ATP synthase (Ahmad and Senior, 2004a, 2005b, 2006). Today we can add αSer-347 to our list of known phosphate binding residues (Li *et al.*, 2009).

Future Directions

Phosphate analog and DCCD assays have not yet been performed on the αThr-349 and βArg-182 mutants, and most assays performed and discussed in Chapter 3 need more replicates. Fluorescence studies should be performed on the newly developed mutants in order to access the effect of mutations on protein folding. Mutations for the remaining residues in the VISIT-DG sequence have been constructed and need to be analyzed as well. These mutations are shown in Appendix E.

All of the assays used for this work measure ATPase activity, and the assay for P_i binding is an indirect measurement. A direct P_i binding assay would enhance these studies greatly because synthesis and hydrolysis reactions are not one in the same. Weber and Senior (2000) state that little is known about ATP synthesis. The mechanism by which ADP and P_i bind is not understood (Weber and Senior, 2000). ATP synthesized can be measured through the use of the bioluminescent luciferin/luciferase assay (Dupaix *et al.,* 1989; Itoh *et al.*, 2004). Investigation of the effect of VISIT-DG mutations on ATP synthesis through the use of the luciferin/luciferase system may help to understand the structural and functional differences between ATP synthesis and ATPase activity.

REFERENCES

"The Nobel Prize in Chemistry 1997". Nobelprize.org. Accessed Sep. 23, 2010. http://nobelprize.org/nobel_prizes/chemistry/laureates/1997/

Abrahams, J. P., Leslie, A. G. W., Lutter, R., and Walker, J. E. (1994) Structure at 2.8 Å Resolution of F_1-ATPase from Bovine Heart Mitochondria. *Nature* **370,** 621-628

Adachi, K., Oiwa, K., Nishizaka, T., Furuike, S., Noji, H., Itoh, H., Yoshida, M., and Kinosita, K. (2007) Coupling of Rotation and Catalysis in F_1-ATPase Revealed by Single-Molecule Imaging and Manipulation. *Cell* **130,** 309-321

Agilent Technologies. QuikChange Lightning Multi Site-Directed Mutagenesis Kit Instruction Manual Catalog # 210513 and #210515 Revision B. Accessed Sep., 2010. http://www.genomics.agilent.com/files/Manual/210513.pdf

Ahmad, Z., and Senior, A. E. (2004a) Mutagenesis of Residue βArg-246 in the Phosphate-Binding Subdomain of Catalytic Sites of *Escherichia coli* F_1-ATPase. *J. Biol. Chem.* **279,** 31505-31513

Ahmad, Z., and Senior, A. E. (2004b) Role of βAsn-243 in the Phosphate-Binding Subdomain of Catalytic Sites of *Escherichia coli* F_1-ATPase. *J. Biol. Chem.* **279,** 46057-46064

Ahmad, Z., and Senior, A. E. (2005a) Modulation of Charge in the Phosphate Binding Site of *Escherichia coli* ATP Synthase. *J. Biol. Chem.* **280,** 27981-27989

Ahmad, Z., and Senior, A. E. (2005b) Involvement of ATP Synthase Residues αArg-376, βArg-182, and βLys-155 in Pi Binding. *FEBS Lett.* **579,** 523-528

Ahmad, Z., and Senior, A. E. (2005c) Identification of Phosphate Binding Residues of *Escherichia coli* ATP Synthase. *J. Bioenerg. Biomembr.* **37,** 437-440

Ahmad, Z., and Senior, A. E. (2006) Inhibition of the ATPase activity of *Escherichia coli* ATP synthase by Magnesium Fluoride. *FEBS Lett.* **580,** 517-520

Al-Shawi, M. K., Parsonage, D., and Senior, A. E. (1990) Thermodynamic Analyses of the Catalytic Pathway of F_1-ATPase from *Escherichia coli*. Implications Regarding the Nature of Energy Coupling by F_1-ATPases. *J. Biol. Chem.* **265,** 4402-4410

Al-Shawi, M. K., and Senior, A. E. (1992) Effects of Dimethyl Sulfoxide on Catalysis in *Escherichia coli* F_1-ATPase. *Biochemistry* **31,** 886-891

Al-Shawi, M. K., Ketchum, C. J., and Nakamoto, R. K. (1997) The *Escherichia coli* F_OF_1 γM23K Uncoupling Mutant Has a Higher K0.5 for Pi. Transition State Analysis of This Mutant and Others Reveals That Synthesis and Hydrolysis Utilize the Same Kinetic Pathway. *Biochemistry* **36,** 12961-12969

Andries, K., Verhasselt, P., Guillemont, J., Gohlmann, H. W. H., Neefs, J.-M., Winkler, H., Van Gestel, J., Timmerman, P., Zhu, M., Lee, E., Williams, P., de Chaffoy, D., Huitric, E., Hoffner, S., Cambau, E., Truffot-Pernot, C., Lounis, N., and Jarlier, V. (2005) A Diarylquinoline Drug Active on the ATP Synthase of *Mycobacterium tuberculosis. Science* **307,** 223-227

Bald, D., Amano, T., Muneyuki, E., Pitard, B., Rigaud, J.-L., Kruip, J., Hisabori, T., Yoshidai, M., and Shibata, M. (1998) ATP Synthesis by F_0F_1-ATP Synthase Independent of Noncatalytic Nucleotide Binding Sites and Insensitive to Azide Inhibition. *J. Biol. Chem.* **273,** 865-870

Berman, H. M., Westbrook, J., Feng, Z., Gilliland, G., Bhat, T. N., Weissig, H., Shindyalov, I. N., Bourne, P. E. (2000) The Protein Data Bank Nucleic Acids Research, **28,** 235-242. Accessed Oct., 2010. www.pdb.org

Bowler, M. W., Montgomery, M. G., Leslie, A. G., and Walker, J. E. (2006) How Azide Inhibits ATP Hydrolysis by the F-ATPases. *Proc. Natl. Acad. Sci. U. S. A.* **103,** 8646-8649

Boyer, P. D. (1979) The Binding - Change Mechanism of ATP Synthesis. Membrane Bioenergetics (Lee, C. P., Schatz, G., and Ernster, L., eds) pp. 461-479, Addison-Wesley, Reading, MA

Boyer, P. D. (1989) A Perspective of the Binding Change Mechanism for ATP Synthesis. *FASEB J.* **3,** 2164-2178

Boyer, P. D. (1997) The Atp Synthase—A Splendid Molecular Machine. *Annu. Rev. Biochem.* **66,** 717-749

Boyer, P. D. (2002) A Research Journey with ATP Synthase. *J. Biol. Chem*. **277,** 39045-39061

Bradford, M. M. (1976) A Rapid and Sensitive Method for the Quantitation of Microgram Quantities of Protein Utilizing the Principle of Protein-Dye Binding. *Anal. Biochem.* **72,** 248-254

Braig, K., Menz, R. I., Montgomery, M. G., Leslie, A. G. W., and Walker, J. E. (2000) Structure of Bovine Mitochondrial F_1-ATPase inhibited by Mg^{2+} ADP and Aluminium Fluoride. *Structure* **8,** 567-573

Brudecki, L. E., Grindstaff, J. J., and Ahmad, Z. (2008) Role of αPhe-291 Residue in the Phosphate-Binding Subdomain of Catalytic Sites of *Escherichia coli* ATP Synthase. *Arch. Biochem. Biophys.* **471,** 168-175

Cabezon, E., Montgomery, M. G., Leslie, A. G. W., Walker, J. E. (2003) The Structure of Bovine F_1-ATPase in Complex with its Regulatory Protein IF_1. *Nature Structural Biology* **10,** 744-750

Chen, C., Saxena, A. K., Simcoke, W. N., Garboczi, D. N., Pedersen, P. L., and Ko, Y. H. (2006) Mitochondrial ATP Synthase. Crystal Structure of the Catalytic F_1 Unit in a Vanadate-Induced Transition-Like State and Implications for Mechanism. *J. Biol. Chem.* **281,** 13777-13783

Chi, S. L., and Pizzo, S. V. (2006) Angiostatin is Directly Cytotoxic to Tumor Cells at Low Extracellular pH: A Mechanism Dependent on Cell Surface–Associated ATP Synthase. *Cancer Res* **66,** 875-882

Cloud, P. E., Licari, G. R., Wright, L. A., and Troxel, B.W. (1969) Proterozoic Eucaryotes from Eastern California. *Proc. Natl.Acad. Sci. U. S. A*. **62,** 623-630

Cole, S. T., and Alzari, P. M. (2005) TB--A New Target, a New Drug *Science* **307,** 214-215

Csondes, A. (2004) Environmental Fate of Methoprene. Environmental Monitoring Branch, Department of Pesticide Regulations, Sacramento, CA, USA. Accessed Nov., 2010. http://www.cdpr.ca.gov/docs/emon/pubs/methofate.pdf

Dadi, P. K., Ahmad, M., and Ahmad, Z. (2009) Inhibition of ATPase Activity of *Escherichia coli* ATP Synthase by Polyphenols. *Int. J. Biol. Macromol.* **45,** 72-79

Davies, J., and Jacob, F. (1968) Genetic Mapping of the Regulator and Operator Genes of the Lac Operon. *J. Mol. Biol.* **36,** 413-417

Deamer, D. W. (2008) Origins of Life: How Leaky Were Primitive Cells? *Nature* **454,** 37-38

De Duve, C. (2002) Life Evolving. New York: Oxford University Press.

De Duve, C. (2005) Singularities. Cambridge: Cambridge University Press.

Devenish, R. J., Prescott, M., Roucou, X., and Nagley, P. (2000) Insights into ATP Synthase Assembly and Function Through the Molecular Genetic Manipulation of Subunits of the Yeast Mitochondrial Enzyme Complex. *Biochim Biophys Acta* **1458,** 428-442

Diez, M., Zimmerman, B., Börsch, M., König, M., Schweinberger, E., Steigmiller, S., Reuter, R., Felekyan, S., Kudryavtsev, V., Seidel, C. A. M., and Gräber, P. (2004) Proton-Powered Subunit Rotation in Single Membrane-Bound F_0F_1-ATP Synthase. *Nat. Struct. Mol. Biol.* **11,** 135-141

Dupaix, A., Johannina, G., and Arrioa, B. (1989) ATP Synthesis and Pyrophosphate-Driven Proton Transport in Tonoplast-Enriched Vesicles Isolated from *Catharanthus roseus. FEBS Lett.* **249,** 13-16.

Feniouk, B. A. A brief history of ATP synthase research. Accessed Sep. 2010. www.atpsynthase.info

Ferguson, S. J., Lloyd, W. J., Lyons, M. H., and Radda, G. K. (1975a) The Mitochondrial ATPase. Evidence for a Single Essential Tyrosine Residue. *Eur. J. Biochem.* **54,** 117-126

Ferguson, S. J., Lloyd, W. J., and Radda, G. K. (1975b) The Mitochondrial ATPase. Selective Modification of a Nitrogen Residue in the Beta Subunit. *Eur. J. Biochem*. **54,** 127-133

Fillingame, R. H. (1990) *The Bacteria*, Vol. XII, (Krulwich, T. A., ed.), pp. 345-391, Academic Press, Orlando, FL.

Frasch, W. D. (2000) The Participation of Metals in the Mechanism of the F_1-ATPase. *Biochim. Biophys. Acta* **1458,** 310-325

Gledhill, J. R., Montgomery, M. G., Leslie, A. G. W., and Walker, J. E. (2007) Mechanism Of Inhibition Of Bovine F_1-Atpase by Resveratrol and Related Polyphenols. *Proc. Natl. Acad. of Sci.* **104,** 13632-13637

Goodsell, D. S. (2005) ATP Synthase RCSB PDB Molecule of the Month. Accessed Nov., 2010. http://dx.doi.org/10.2210/rcsb_pdb/mom_2005_12

Green, A. A. (1933) The Preparation of Acetate and Phosphate Buffer Solutions of Known PH and Ionic Strength. *J. Am. Chem. Soc*. **55,** 2331-2336.

Haldane, J. B. S. (1929) The Origin of Life. *Rationalist Annual* **3,** 3-10

Häse, C. C., Fedorova, N. D., Galperin, M. Y., and Dibrov, P. A. (2001) Sodium Ion Cycle in Bacterial Pathogens: Evidence from Cross-Genome Comparisons. *Microbiol Mol Biol Rev*. **65,** 353–370

Hermolin, J., and Fillingame, R. H. (1989) H^+-ATPase Activity of *Escherichia coli* F_1F_0 is Blocked After Reaction of Dicyclohexylcarbodiimide with a Single Proteolipid (Subunit *c*) of the F_0 Complex. *J. Biol. Chem.* **264,** 3896-3908

Hong, S., and Pedersen, P. L. (2008) ATP Synthase and the Actions of Inhibitors Utilized to Study Its Roles in Human Health, Disease, and Other Scientific Areas. *Microbiol. Mol. Biol. Rev.* **72,** 590-641

Itoh, H., Takahashi, A., Adachi, K., Noji, H., Yasuda, R., Yoshida, M., and Kinosita, K. (2004) Mechanically Driven ATP Synthesis by F_1-ATPase. *Nature* **427,** 465-468

Karrasch, S., and Walker, J. E. (1999) Novel Features in the Structure of Bovine ATP Synthase. *J. Mol. Biol.* **290,** 379-384

Ketchum, C. J., Al-Shawi, M. K., and Nakamoto, R. K. (1998) Intergenic Suppression of the GammaM23K Uncoupling Mutation in F_0F_1 ATP Synthase by BetaGlu-381 Substitutions: The Role of the Beta380DELSEED386 Segment in Energy Coupling. *Biochem. J.* **330,** 707-712

Klionsky, D. J., Brusilow, W. S. A., and Simoni, R. D. (1984) *In Vivo* Evidence for the Role of the Epsilon Subunit as an Inhibitor of the Proton-Translocating ATPase of *Escherichia coli*. *J. Bacteriol.* **160,** 1055-1060

Kolodziejczyk, R., Bujacz, G., Jakób, M., Ożyhar, A., Jaskolski, M., and Kochman, M. (2008) Insect Juvenile Hormone Binding Protein Shows Ancestral Fold Present in Human Lipid-Binding Proteins. *J. Mol. Biol.* **377,** 870-881

Kresge, N., Simoni, R. D., and Hill, R. L. (2006) Unraveling the Enzymology of Oxidative Phosphorylation: The Work of Efraim Racker. *J. Biol. Chem*. **281,** e4-e6

Laemmli, U. K. (1970) Cleavage of Structural Proteins During the Assembly of the Head of Bacteriophage T4. *Nature* **227,** 680-685

Lane, N., Allen, J. F., Martin, W. (2010) How Did LUCA Make a Living? Chemiosmosis in the Origin of Life. *BioEssays* **32,** 271-280

Langen, P., and Hucho, F. (2008) Karl Lohmann and the Discovery of ATP. *Angew.*

Chem. Int. Ed. **47,** 1824–1827

Li, W., Brudecki, L. E., Senior, A. E., and Ahmad, Z. (2009) Role of α-Subunit VISIT-DG Sequence Residues Ser-347 and Gly-351 in the Catalytic Sites of *Escherichia coli* ATP Synthase. *J. Biol. Chem.* **284,** 10747-10754

Löbau, S., Weber, J., and Senior, A. E. (1998) Catalytic Site Nucleotide Binding and Hydrolysis in F_1F_o-ATP Synthase. *Biochemistry* **37,** 10846-10853

Martin, W. and Muller, M. (1998) The Hydrogen Hypothesis for the First Eukaryote. *Nature* **392,** 37-41

Menz, R. I., Walker, J. E., and Leslie, A. G. W. (2001) Structure of Bovine Mitochondrial F_1-ATPase with Nucleotide Bound to All Three Catalytic Sites. *Cell* **106,** 331-341

Mitchell, P. (1961) Coupling of Phosphorylation to Electron and Hydrogen Transfer by a Chemi-Osmotic Type of Mechansim. *Nature* **191,** 144-148

Mitchell, P. (1978) David Keilin's Respiratory Chain Concept and its Chemiosmotic Consequences. *Nobel Lectures, Chemistry* 1971-1980, Editor-in-Charge Tore Frängsmyr, Editor Sture Forsén, World Scientific Publishing Co., Singapore, 1993, 295-330

Mulkidjanian, A. Y., Makarova, K. S., Galperin, M. Y., and Koonin, E. V. (2007) Inventing the Dynamo Machine: the Evolution of the F-type and V-type ATPases. Nature Reviews: *Microbiology.* **5,** 892-899.

Mulkidjanian, A. Y., Dibrovc, P., and Galperind, M. Y. (2008) The Past and Present of Sodium Energetics: May the Sodium-Motive Force Be With You. *Biochim Biophys Acta*. **1777,** 985-992

Mulkidjanian, A. Y., Galperin, M.Y., and Koonin, E. V. (2009) Co-Evolution of Primordial Membranes and Membrane Proteins. *Trends Biochem Sci*. **34,** 206-215

Nadanaciva, S., Weber, J., and Senior, A. E. (1999) Binding of the Transition State Analog MgADP-Fluoroaluminate to F_1-ATPase. *J. Biol. Chem.* **274,** 7052-7058

Nadanaciva, S., Weber, J., and Senior, A. E. (2000) New Probes of the F_1-ATPase Catalytic Transition State Reveal That Two of the Three Catalytic Sites Can Assume a Transition State Conformation Simultaneously. *Biochemistry* **39,** 9583-9590

Nakamoto, R. K., Baylis Scanlon, J. A., Al-Shawi, M. K. (2008) The Rotary Mechanism of ATP Synthase. *Arch Biochem Biophys.* **476,** 43-50

Nanomedicine Overview. (2010) National Institutes of Health. Division of Program Coordination, Planning, and Strategic Initiatives. Bethesda, Maryland, USA. Accessed Nov., 2010. http://nihroadmap.nih.gov/nanomedicine/

Nelson, D. L., and Cox, M. M. (2005) Lehninger Principles of Biochemistry. 4th ed. W.H. Freeman and Company. pp. 690-750.

Noji, H., Yasuda, R., Yoshida, M., and Kinosita, K. Jr. (1997) Direct Observation of the Rotation of F_1-ATPase. *Nature* **386,** 299-302

Noji, H., and Yoshida, M. (2001) The Rotary Machine in the Cell, ATP Synthase. *J. Biol. Chem.* **276,** 1665-1668

Orriss, G. L., Leslie, A. G. W., Braig, K., and Walker, J E. (1998) Bovine F_1-ATPase Covalently Inhibited with 4-chloro-7-nitrobenzofurazan: The Structure Provides Further Support for a Rotary Catalytic Mechanism. *Structure* **6,** 831-837

Pedersen, P. L. (2005) Transport ATPases: Structure, Motors, Mechanism and Medicine: A Brief Overview. *J. Bioenerg. Biomembr.* **37,** 349-357

Penefsky, H. S., Pullman, M. E., Datta, A., and Racker, E. (1960) Partial Resolution of the Enzymes Catalyzing Oxidative Phosphorylation: II. Participation of a Soluble Adenosine Triphosphatase in Oxidative Phosphorylation. *J. Biol. Chem.* **235,** 3330-3336

Penefsky, H. S. (2005) Pi binding by the F_1-ATPase of Beef Heart Mitochondria and of the Plasma Membrane. *FEBS Lett.* **579,** 2250-2252

Perez, J. A., Greenfield, A. J., Sutton, R., and Ferguson, S. J. (1986) Characterisation of Phosphate Binding to Mitochondrial and Bacterial Membrane-Bound ATP Synthase by Studies of Inhibition with 4-chloro-7-nitrobenzofurazan. *FEBS Lett.* **198,** 113-118

Petermann, I., Huebner, C., Browning, B. L., Gearry, R. B., Barclay, M. L., Kennedy, M., Roberts, R., Shelling, A. N., Philpott, M., Han, D. Y., and Ferguson, L. R. (2009) Interactions Among Genes Influencing Bacterial Recognition Increase IBD Risk in a Population-Based New Zealand Cohort. *Human Immunology* **70,** 440-446

Prebble, J. N. (1996) Successful Theory Development in Biology: A Consideration of the

Theories of Oxidative Phosphorylation Proposed by Davies and Krebs, Williams and Mitchell. *Biomedical and Life Sciences Bioscience Reports.* **16,** 207-215.

Poole, A. M., Jeffares, D. C., and Penny, D. (1998) The Path from the RNA World. *J. Mol. Evol.* **46,** 1-17

Pullman, M. E., Penefsky, H. S., Datta, A., and Racker, E. (1960) Partial Resolution of the Enzymes Catalyzing Oxidative Phosphorylation: I. Purification and Properties of Soluble, Dinitrophenol-Stimulated Adenosine Triphosphatase. *J. Biol. Chem.* **235,** 3322-3329

Qi, S.-Y., Li, Y., Szyroki, A., Giles, I. G., Moir, A., O'Connor, C. D. (1995) *Salmonella typhimurium* Responses to a Bactericidal Protein from Human Neutrophils. *Molecular Microbiology.* **17,** 523-531

Rao, R., Perlin, D. S., and Senior, A. E. (1987) The Defective Proton-ATPase of UncA Mutants of *Escherichia coli*: ATP-Binding and ATP-Induced Conformational Change in Mutant α-Subunits. *Arch. Biochem. Biophys.* **255,** 309-315

Ren, H., and Allison, W. S. (2000) On What Makes the Gamma Subunit Spin During ATP Hydrolysis by F_1. *Biochim. Biophys. Acta* **1458,** 221-233

Schagger, H., and Ohm, T. G. (1995) Human Diseases with Defects in Oxidative Phosphorylation. *Eur J Biochem* **227,** 916-921

Segré, D., Ben-Eli, D., Deamer, D. W., and Lancet, D. (2001) The Lipid World. *Orig. Life Evol. Biosph.* **31,** 119-145.

Senior, A. E. (1988) ATP Synthesis by Oxidative Phosphorylation. *Physiol. Rev.* **68,** 177-231

Senior, A. E., Langman, L., Cox, G. B., and Gibson, F. (1983) Oxidative Phosphorylation in *Escherichia coli*. Characterization of Mutant Strains in which F_1-ATPase Contains Abnormal Beta-Subunits. *Biochem. J.* **210,** 395-403

Senior, A. E., Latchney, L. R., Ferguson, A. M., and Wise, J. G. (1984) Purification of F_1-ATPase with Impaired Catalytic Activity from Partial Revertants of *Escherichia coli* UncA Mutant Strains. *Arch. Biochem. Biophys.* **228,** 49-53

Senior, A. E., Nadanaciva, S., and Weber, J. (2002) The Molecular Mechanism of ATP Synthesis by F_1F_0-ATP Synthase. *Biochim. Biophys. Acta.* **1553,** 188-211

Szostak, J.W., Bartel, D. P., and Luisi, P. L. (2001) Synthesizing Life. *Nature* **409,** 387-390

Takahashi, K., Jiang, X.-C., Sakai, N., Yamashita, S., Hirano, K., Bujo, H., Yamazaki, H., Kusunoki, J., Miura, T., Kussie, P., Matsuzawa, Y., Saito, Y., Tall, A. (1993) A Missense Mutation in the Cholesteryl Ester Transfer Protein Gene with Possible Dominant Effects on Plasma High Density Lipoproteins. *J. Clin. Invest.* **92,** 2060-2064

Taussky, H. H., and Shorr, E. (1953) A Microcolorimetric Method for the Determination of Inorganic Phosphorus. *J. Biol. Chem.* **202,** 675–685

Thorburn, D. R., Rahman, S. Mitochondrial DNA-Associated Leigh Syndrome and NARP. Pagon RA, Bird TC, Dolan CR, Stephens K, editors. GeneReviews [Internet]. Seattle (WA): University of Washington, Seattle; 1993-2003 Oct 30 [updated 2006 Sep 22]. Accessed Oct., 2010. PMID: 20301352. http://www.ncbi.nlm.nih.gov/pubmed/20301352

Tombline, G., Bartholomew, L., Gimi, K., Tyndall, G. A., and Senior, A. E. (2004) Synergy Between Conserved ABC Signature Ser Residues in P-Glycoprotein Catalysis. *J. Biol. Chem.* **279,** 5363-5373

Vandeyar, M. A., Weiner, M. P., Hutton, C. J., and Batt, C. A. (1988) A Simple and Rapid Method for the Selection of Oligodeoxynucleotide-Directed Mutants. *Gene* **65,** 129-133

Vlassov, A. (2005) How Was Membrane Permeability Produced in an RNA world? *Orig. Life Evol. Biosph*. **35,** 135-149

Wade, L. A., Fraser, S., Haile, S., Collier, P. (2010) An Approach to Mimicking Abiotic Hydrogenation of Carbon Dioxide in Alkaline Hydrothermal Vents. Astrobiology Science Conference 2010. Accessed Oct. 26, 2010. http://www.lpi.usra.edu/meetings/abscicon2010/pdf/5646.pdf

Walker, J. E., Saraste, M., Runswick, M. J., and Gay, N. J. (1982) Distantly Related Sequences in the a- and f-subunits of ATP synthase, Myosin, Kinases and Other ATP-Requiring Enzymes and a Common Nucleotide Binding Fold. *The EMBO Joumal* **1,** 945-951

Wallace, D. C. (1999) Mitochondrial Diseases in Man and Mouse. *Science* **283,** 1482-1488

Weber, J. (2007) ATP Synthase – The Structure of the Stator Stalk. *Trends. Biochem. Sci.* **32,** 53-56

Weber, J., and Senior, A. E. (1995) Location and Properties of Pyrophosphate-Binding Sites in *Escherichia coli* F_1-ATPase. *J. Biol. Chem.* **270,** 12653-12658

Weber, J., and Senior, A. E. (1997) Catalytic Mechanism of F_1-ATPase. *Biochim. Biophys. Acta* **1319,** 19–58

Weber, J., and Senior, A. E. (2000) ATP synthase: What We Know About ATP Hydrolysis and What We Do Not Know About ATP Synthesis. *Biochem. Biophys. Acta* **1458,** 300-309

Weber, J., and Senior, A. E. (2003) ATP Synthesis Driven by Proton Transport in F_1F_0-ATP Synthase. *FEBS Lett.* **545,** 61-70

Weber, J., Hammond, S. T., Wilke-Mounts, S., and Senior, A. E. (1998) Mg^{2+} Coordination in Catalytic Sites of F_1-ATPase. *Biochemistry* **37,** 608-614

Weber, J., Wilke-Mounts, S., and Senior, A. E. (1994) Cooperativity and Stoichiometry of Substrate Binding to the Catalytic Sites of *Escherichia coli* F_1-ATPase. Effects of Magnesium, Inhibitors, and Mutation. *J. Biol. Chem.* **269,** 20462-20467

Weber, J., Wilke-Mounts, S., Lee, R. S. F., Grell, E., and Senior, A. E. (1993) Specific Placement of Tryptophan in the Catalytic Sites of *Escherichia coli* F_1-ATPase Provides a Direct Probe of Nucleotide Binding: Maximal ATP Hydrolysis Occurs with Three Sites Occupied. *J. Biol. Chem.* **268,** 20126-20133

Whitesides, G. M. (2003) The 'Right' Size in Nanobiotechnology. *Nat Biotechnol.* **21,** 1161-1165

Xing, S.-L., Yan, J., Yu, Z.-H., Zhu, C.-Q. (2010) Neuronal Cell Surface ATP Synthase Mediates Synthesis of Extracellular ATP and Regulation of Intracellular pH. *Cell Biol Int*. Immediate Publication, doi:10.1042/CBI20090441. Accesses Nov., 2010. http://www.cellbiolint.org/cbi/imps/pdf/CBI20090441.pdf

Yoshida, M., Allison, W. S., Esch, F. S., and Futai, M. (1982) The Specificity of Carboxyl Group Modification During the Inactivation of the *Escherichia coli* F_1-ATPase with Dicyclohexyl[^{14}C]carbodiimide. *J. Biol. Chem.* **257,** 10033-10037

Zalewska, M., Kochmanb, A., Estèvec, J.-P., Lopezc, F., Chaouid, K., Susinic, C., Ożyhara, A., and Kochman, M. (2009) Juvenile hormone binding protein traffic — Interaction with ATP synthase and lipid transfer proteins. *Biochimica et Biophysica Acta* **1788,** 1695-1705

Zhang, L.-H., Kamanna, V. S., Zhang, M. C., and Kashyap, M. L. (2008) Niacin Inhibits Surface Expression of ATP Synthase β Chain in HepG2 Cells: Implications for Raising HDL. *Journal of Lipid Research* **49,** 1195-1201

APPENDICES

Appendix A

Buffers and Reagents

50 mM Tris-SO_4 buffer

- To 90 ml H_2O add
- 0.61 g Tris
- Adjust pH to 8.0 with 6M H_2SO_4
- Bring to a final volume of 100 ml with H_2O

ATPase cocktail

- In 150 ml H_2O add
- 10 ml 1 M Tris
- 0.8 ml 1M $MgCl_2$
- 5 ml 0.4 NaATP (Adenosine 5'-triphosphate disodium salt)
    - Add NaATP slowly to H_2O while maintaining pH 5-9 with 6M NaOH.
- Adjust pH to 8.5 with 6M H_2SO_4
- Bring to a final volume of 200 ml with H_2O
- Freeze in plastic bottles at -20°C

10 % SDS

- 100 g sodium dodecyl sulfate
- Bring to a final volume of 1000 ml with H_2O

Taussky and Shorr (T&S) reagent

- Sol A: 1.2 g ammonium molybdate ($(NH_4)6Mo_7O_{24}\cdot 4H_2O$ in 9.8 ml 12 N H_2SO_4)
- Sol B: 10 g ferrous ammonium sulfate ($Fe(NH_4)2(SO_4)_2\cdot 6H_2O$ in 70 ml H_2O)
- Add sol A to sol B while stirring
- Bring to a final volume of 100 ml with H_2O
- Store at 4°C

STEM

- To 700 ml H_2O add
- 100 ml 1 M TES
- 4.29 g $Mg(CH_3CO_2)_2\cdot 4H_2O$
- 85.5 g sucrose
- 0.0951 g EGTA (ethylene glycol-bis(2-aminoethylether)-N,N,N,N-tetraacetic acid)
- 5 g EACA (6-aminocaproic acid)
- Adjust pH to 6.5 with 6M NaOH
- Bring to a final volume of 1000 ml with H_2O
- Freeze in plastic bottles at -20°C

TES 50

- To 700 ml H_2O add
- 50 ml 1 M TES
- 150 ml glycerol
- 5 g EACA (6-aminocaproic acid)
- 1 g PAB (4-aminobenzamidine dihydrochloride)
- Adjust pH to 6.5 with 6M NaOH
- Bring to a final volume of 1000 ml with H_2O
- Freeze in plastic bottles at -20°C

TES 5 + PAB

- To 700 ml H_2O add
- 5 ml 1 M TES
- 150 ml glycerol
- 1 ml 0.5 M DTT (dithiothreitol)
- 5 g EACA (6-aminocaproic acid)
- 1 g PAB (4-aminobenzamidine dihydrochloride)
- 2.5 ml 0.2 M EDTA (ethylenediaminetetraacetic acid disodium salt dihydrate)
- Adjust pH to 6.5 with 6M NaOH
- Freeze in plastic bottles at -20°C

AET (argenine ent thiamine)

- To 60 ml H_2O add
- 0.617 g 2,3 dihydroxy benzoic acid
- 16.86 g L-arginine HCl
- 1 ml 20 mM thiamine
- Add just enough amount of 1M NaOH to dissolve everything
- Make final volume to 100 ml with H_2O
- Filter sterilize

TE (trace elements)

- To 80 ml H_2O
- 0.251 g zinc sulfate ($ZnSO_4.7H_2O$)
- 0.017 g manganese sulfate ($MnSO_4.H_2O$)
- 0.029 g boric acid (H_3BO_3)
- 0.012 g calcium sulfate ($CaSO_4.2H_2O$)
- 0.037 g calcium chloride ($CaCl_2.2H_2O$)
- 0.049 g ferric chloride ($FeCl_3.6H_2O$)
- Make final volume to 100 ml with H_2O.
- Filter sterilize

ILV (isoleucine-valine)

- To 95 ml H_2O add
- 0.394 g isoleucine
- 0.352 g valine
- Make final volume to 100 ml with H_2O
- Filter sterilize

Potassium phosphate buffer (0.1 M) pH 7.2 (Green, 1933)

- 71.7 ml 1 M K_2HPO_4
- 28.3 ml 1 M KH_2PO_4
- Dilute the 1M stock solution to 1000 ml with distilled H_2O. pH may be calculated using the Henderson-Hasselbalch equation.

Appendix B

Culture Media and Plates

LB liquid medium

- 12.5 g of LB broth powder
- Add H_2O to bring to 500 ml
- Autoclave for 30 minutes
- Cool the media to ~50°C
- Add 500 µl of 100 mg/ml Ampicillin

Minimal glucose

- Minimal media
    - To 400 ml H_2O add
    - 5.225 g potassium phosphate dibasic (K_2HPO_4)
    - 2.40 g sodium phosphate monobasic (NaH_2PO_4)
    - 0.99 g ammonium sulfate ($(NH_4)_2SO_4$)
    - Autoclave for 30 min, cool to room temperature
- Additions
    - 10 ml uracil
    - 1 ml 27 % glucose (3 mM)
    - 5 ml isoleucin-valine (ILV)
    - 0.5 ml trace elements (TE)
    - 0.5 ml 1 M magnesium sulfate ($MgSO_4$)
    - 0.5 ml argenine ent thimine (AET)
    - 0.5 ml 100 mg/ml ampicillin
    - 3.12 ml 4X LB

LB-agar plate with ampicillin

- 12.5g of LB broth powder
- 7.5g of agar
- Bring to a final volume of 500 mL with H_2O
- Autoclave for 30 minutes
- Cool the media to ~50°C
- Add 500 µl of 100 mg/ml ampicillin
- Pour into sterile plates

Succinate Broth

- Prepare 500 ml minimal media
- Additions
    - 10 ml uracil
    - 10 ml 17.7% succinate
        - To 300 ml H_2O add
            - 88.5 g succinic acid
            - 50 g NaOH

        - Adjust to pH 7.0, bring to 500 ml, and autoclave
        - This solution becomes hot when dissolving: stir in an ice bath.
    - 0.5 ml TE
    - 0.5 ml 1 M $MgSO_4$
    - 0.5 ml AET
    - 5 ml 6% casamino acids (CAS) optional
    - 0.5 ml 100 mg/ml ampicillin

Appendix C

Membrane Preparation and ATPase Assays

Membrane preparation

Starter Culture: Make using aseptic technique. Always perform limiting glucose and succinate growth curves before preparing membranes (Mbr).

DAY 1:

Prepare solutions. Inoculate LB broth tubes with a single colony and grow O/N (16-20 hrs) at 37°C and 250 RPM in water/air shaker.

DAY 2:

1. Prepare duplicate starter culture flasks.
   a) Prepare minimal media (MM) in one large batch. Dissolve and separate into 250 mL flasks with 50 mL each. Cap each flask with foam and aluminum foil. Autoclave on liquid cycle for 20-30 min.
   b) Once 50 mL MM has cooled, make the following additions:
      1. 50 µl TE
      2. 50 µl 1 M $MgSO_4$
      3. 50 µl AET
      4. 50 µl ampicillin (100 mg/mL) or 100 µl ampicillin (50 mg/mL)
      5. 1 mL 27% glucose (30 mM)
      6. 1 mL 0.11% uracil
      7. 500 µl IlV
      8. 312 µl 4XLB (2.5% LB in final volume)
2. Inoculate each 50 mL flask with 10-15 µl of LB amp broth which has been previously grown O/N (16-20 hrs) at 37°C, 250 RPM.
3. Grow in 37°C water/air shaker at 250 RPM for 6-8 hours.
4. Once the 50 mL flasks have grown for 6-8 hours, they will be used as the inoculums for the 1 L flasks.
5. To the 1L MM flask, make the following additions:
      1. 1000µl TE
      2. 1000µl 1M $MgSO_4$
      3. 1000µl AET
      4. 1000µl ampicillin (100 mg/mL) or 2000 µl ampicillin (50 mg/mL)
      5. 20 mL 27% glucose
      6. 20 mL 0.11% uracil
      7. 10 mL IlV
      8. 6240µl 4XLB
6. Grow in 37°C water/air shaker at 250 RPM for 6-8 hours. Read OD_{595} every hour until late log phase. Sometimes longer than 8 hours is required for mutants.
7. Go to harvesting cells.

Harvesting Cells: All steps below should be on ice or at 2°C.

1. Spin suspension with Super Speed RC5B centrifuge in a Sorvall GSA rotor at 9500 RPM X 15 min in 250 mL polycarbonate bottles.
2. Resuspend combined pellets in STEM at 2°C using clean paint brush (rinse with dH_2O).
3. Spin at 9500 RPM for 25 min. Aim to combine pellets in same container throughout the next few steps.
4. Weigh pellet by difference and resuspend pellet in 2 mL STEM/g wet cells. Freeze bottle with cells in -80°C overnight or proceed directly to next step. Do not store longer than overnight.

DAY 3:

French Press and TES 50 Wash:

1. Thaw cells on ice. Add 15-20 mg of DNAse (Deoxyribonuclease I from bovine pancreas) to the thawed pellet.
2. Slowly pass through chilled French press twice at 20K psi.
3. Spin with ultra-centrifuge WX80 in 65 Ti rotor at 22K RPM for 20 min for DK8: for other strains spin at 18K RPM for 20 min.
4. Discard pellet and spin supernatant at 60K RPM for 2 hr at 2°C. Fill tubes with STEM.
5. Resuspend pellets in TES 50 with paint brush.
6. Spin at 60K RPM for 2hr at 2°C.
7. Discard supernatant. Freeze pellets (in tube) in -80°C or go to next step.

TES 5 + PAB Wash:

1. Thaw pellet on ice.
2. Resuspend pellets in TES 5 + PAB.
3. Spin with ultra-centrifuge WX80 in 65 Ti rotor at 60K RPM for 75-90 min.
4. Repeat steps 2 and 3.
5. Freeze pellet in -80°C, go to F_1 prep (not shown), or go to membrane resuspension.

Membrane Resuspension:

1. Add 500-800 µl 50 mM Tris sulfate pH 8 (T8) to centrifuge tube and resuspend using small paint brush to avoid frothing.
2. Thoroughly resuspend pellet. Transfer to microfuge tube.
3. Final volume of membrane should contain 2.5 mM $MgSO_4$.

4. Store in -20°C for immediate use or in -80°C for longer storage.
5. Find protein concentration using the Bradford method and bovine serum albumin (BSA) as a standard.

ATPase assays

1. According to growth assays, amount and time of reaction will vary.
   In general, the reaction will proceed as follows:

50mM T8 + Mbr + $ATP_{cocktail}$ + 10% SDS + T&S (2-5 min)

2. The blank reaction will proceed as follows:

50mM T8 + Mbr + 10% SDS + $ATP_{cocktail}$ + T&S (2-5 min)

3. Read OD_{700}.
4. For a total reaction volume of 100 µl with a membrane that is 10 µg protein/µl, add 2 µl for 20 µg protein, and 98 µl of T8 for a final volume of 100 µl. Where other solutions are added, the volume of T8 is adjusted to maintain a reaction volume of 100 µl.
5. The ratio of $ATP_{cocktail}$, SDS, and T&S should be 1:1:1.
6. Vortex after addition of each solution.
7. Specific Activity = (Sample OD – Blank OD) / [Amount (mg) X Time (min)]

NOTES:

- Add Mbr to start reaction.
- Assays should be performed in duplicate.
- Membranes should be kept on ice.
- All reactions take place at room temperature.
- To reduce error, make a cocktail of Mbr and T8 and pipette 10 µl per tube.
- After $ATP_{cocktail}$ is thawed in cold water, move it to ice.
- Blanks used for initial, midpoint, and final concentrations unless noted otherwise.
- Volumes and stock solution molarities may have been different than shown in tables.
- Number of tubes needed may vary.

Inhibition by NBD-Cl: Light sensitive: complete reaction in dark.

- Additions of NBD-Cl may not yield an exact µM concentration.
- Blanks for tubes 0, 7, 13.
- NBD-Cl stock and dilutions made in DMSO.

NBD-Cl Stock	Tube #	NBD-Cl (µl)	[NBD-Cl] (µM)	T8 (µl)	Mbr (µl)
	0	0	0	89	10
250 µM	1	2	5	87	10
	2	4	10	85	10
	3	6	15	83	10
	4	8	20	81	10
	5	10	25	79	10
500 µM	6	8	40	81	10
	7	10	50	79	10
2500 µM	8	3	75	86	10
	9	4	100	85	10
	10	6	150	83	10
	11	8	200	81	10
	12	10	250	79	10
	13	12	300	77	10
	14	16	400	73	10

Inhibition by NaN_3:

- Incubate for 30 min with NaN_3

NaN_3 Stock	Tube #	NaN_3 (µl)	NaN_3 (µM)	T8 (µl)	Mbr (µl)
2.5mM	0	0	0	89	10
	1	1	25	88	10
	2	2	50	87	10
	3	4	100	85	10
	4	6	150	83	10
	5	8	200	81	10
	6	10	250	79	10
	7	12	300	77	10
	8	14	350	75	10
	9	16	400	73	10
	10	18	450	71	10
	11	20	500	69	10

Inhibition with an Extra Pulse of NBD-Cl:

- EXAMPLE OF CALCULATIONS:
  - 0.00015M(100 µl) = X µl (0.00052M [stock])
    - 2.885 µl stock NBD-Cl in each tube with reaction volume of 100 µl for 150 µM NBD-Cl.
  - 0.0002M (100 µl) = X µl (0.0052M [stock])
    - 3.846 µl stock NBD-Cl in each tube with reaction volume of 100 µl for 200 µM NBD-Cl.
- Treatment tube:
  50 mM T8 + Mbr + 150 µM NBD-Cl (inc 1h) + 150 µM NBD-Cl (inc 1h) + $ATP_{cocktail}$ + 10% SDS + T&S (2-5 min)
- Blank tube:
  50 mM T8 + Mbr + 150 µM NBD-Cl (inc 1h) + 150 µM NBD-Cl (inc 1h) + 10% SDS + $ATP_{cocktail}$ + T&S (2-5 min)
- One blank for each tube.

Tube #	150 µM NBD-Cl	T8 (µl)	Mbr (µl)	150 µM NBD-Cl
1	2.89 µl 5200 µM stock	86.11	10	NONE
2	2.89 µl 5200 µM stock	86.11	10	3.85 µl 5200 µM stock

DTT Reversibility of NBD-Cl Inhibition:

Tube Number

1. 50 mM T8 + Mbr + $ATP_{cocktail}$ + 10% SDS + T&S (2-5 min)
2. 50 mM T8 + Mbr + 150 µM NBD-Cl (incubate 1h) + $ATP_{cocktail}$ + 10% SDS + T&S (2-5 min)
3. 50 mM T8 + Mbr + 150 µM NBD-Cl (incubate 1h) + 4 mM DTT (inc 1h) + $ATP_{cocktail}$ + 10% SDS + T&S (2-5 min)
4. 50 mM T8 + Mbr + 4 mM DTT (incubate 1h) + $ATP_{cocktail}$ + 10% SDS + T&S (2-5 min)

- DTT stock kept on ice.
- NBD-Cl reaction in dark.
- Blank for each tube.

Tube #	150 µM NBD-Cl	T8 (µl)	Mbr (µl)	4 mM DTT
1	NONE	86.11	10	NONE
2	2.89 µl 5200 µM stock	86.11	10	0.8 µl of 0.5 M stock
3	NONE	86.11	10	0.8 µl of 0.5 M stock
4	2.89 µl 5200 µM stock	86.11	10	NONE

MgADP Protection from NBD-Cl Inhibition:

- Pre-incubate Mbr with MgADP at varying concentrations: 0-12mM (15 mM maximum).
- Mg and ADP concentrations in a ratio of 1:1
    - $MgSO_4$ stock 0.05M
    - NaADP stock 0.05M
- Add 150 µM NBD-Cl in each tube except 0 tubes.
- Blanks for tube 0, 11, and 16.

Tube #	Mg (µl)	ADP (µl)	[MgADP] (µM)	T8 (µl)	Mbr (µl)	150 µM NBD-Cl
0	0	0	0	89	10	0
1	1	1	0.5	87	10	2.88 µl of 5.2 mM stock
2	1.5	1.5	0.75	86	10	
3	2	2	1	85	10	
4	3	3	1.5	83	10	
5	4	4	2	81	10	
6	5	5	2.5	79	10	
7	6	6	3	77	10	
8	7	7	3.5	75	10	
9	8	8	4	73	10	
10	9	9	4.5	71	10	
11	10	10	5	69	10	
12	11	11	5.5	67	10	
13	12	12	6	65	10	
14	14	14	8	61	10	
15	16	16	10	57	10	
16	18	18	12	53	10	

MgPi Protection from NBD-Cl inhibition:

1. Add T8.
2. Add Pi + Mg.
3. Add Mbr.
4. Inc 1h at room temperature.
5. To all, except tube #0, add 2 µl NBD-Cl.
6. At 5 min, 10 min, 15 min…add ATPcocktail.
7. Stop reaction at appropriate time.
8. Read one set at a time.

Tube #	Assay at X min
0	5
1	10
2	15
3	20
4	30
5	30
6	40

SET 1					
Tube #	T8 (µl)	Pi (25 mM)	Mg (25 mM)	Mbr (µl)	NBD-Cl (2.5 mM)
0	40	0	0	10	0
1	38	0	0	10	2
2	38	0	0	10	2
3	38	0	0	10	2
4	38	0	0	10	2
5	38	0	0	10	2
6	38	0	0	10	2
SET 2					
Tube #	T8 (µl)	Pi (25 mM)	Mg (25 mM)	Mbr (µl)	NBD-Cl (2.5 mM)
0	40	0	0	10	0
1	28	5	5	10	2
2	28	5	5	10	2
3	28	5	5	10	2
4	28	5	5	10	2
5	28	5	5	10	2
6	28	5	5	10	2
SET 3					
Tube #	T8 (µl)	Pi (25 mM)	Mg (25 mM)	Mbr (µl)	NBD-Cl (2.5 mM)
0	40	0	0	10	0
1	28	5	5	10	2
2	28	5	5	10	2
3	28	5	5	10	2
4	28	5	5	10	2
5	28	5	5	10	2
6	28	5	5	10	2
SET 4					
Tube #	T8 (µl)	Pi (25 mM)	Mg (25 mM)	Mbr (µl)	NBD-Cl (2.5 mM)
0	40	0	0	10	0
1	28	5	5	10	2
2	28	5	5	10	2
3	28	5	5	10	2
4	28	5	5	10	2
5	28	5	5	10	2
6	28	5	5	10	2

Inhibition by DCCD:

- One 16 h incubation and one 1 h incubation should be performed.
- DCCD stock and dilutions should be made in DMSO.

DCCD Stock	Tube #	DCCD (µl)	[DCCD] (µM)	T8 (µl)	Mbr (µl)
250 µM	0	0	0	89	10
	1	2	5	87	10
	2	4	10	85	10
	3	8	20	81	10
500 µM	4	6	30	83	10
	5	8	40	81	10
	6	10	50	79	10
2500 µM	7	3	75	86	10
	8	4	100	85	10
	9	6	150	83	10
	10	8	200	81	10
	11	10	250	79	10
5000 µM	12	6	300	83	10
	13	8	400	81	10
	14	10	500	79	10

Inhibition by AlF_x:

- First a cocktail needs to be made:
  - 2.5m M $MgSO_4$ (make 1 M stock and store at RT)
  - 10m M NaF (make 1 M stock and store at RT)
  - 1m M NaADP (make 0.5 M stock and store at -20°C)
  - Mbr (add enough so that there is 20 µg/tube)
  - Make final volume with T8
  - Mix by inverting tube
    - Here is an example for 2.5 ml of cocktail
      - 6.5 µl 1 M $MgSO_4$ → 2.6 mM
      - 30 µl 1 M NaF → 12 mM
      - 6 µl 0.449 M NaADP → 1 mM
      - X µl Mbr to get 20-30 µg each tube (25 tubes x 20 µg each→500 µg)
      - V_f with T8
    - For 10ml
      - 26 µl 1 M $MgSO_4$ → 2.6 mM
      - 120 µl 1 M NaF → 12 mM
      - 24 µl 0.449 M NaADP → 1 mM
      - i.e. 100 µl Mbr to get 20-30 µg each tube
      - V_f with T8→9730 µl
- Each tube will have a final volume of 110 µl

AlF_x Stock	Tube #	AlF_x (µl)	[AlF_x] (µM)	T8 (µl)	Cocktail (µl)
	0	0	0	10	100
2.5 mM	1	1	0.0227	9	100
	2	2	0.0455	8	100
	3	3	0.0682	7	100
	4	4	0.09091	6	100
	5	5	0.11364	5	100
	6	6	0.1364	4	100
	7	7	0.1591	3	100
	8	8	0.1818	2	100
25 mM	9	1	0.2273	9	100
	10	1.5	0.34091	8.5	100
	11	2	0.45455	8	100
	12	2.5	0.5682	7.5	100
	13	3	0.68182	7	100
	14	3.5	0.79545	6.5	100
	15	4	0.90911	6	100
	16	5	1.1364	5	100
	17	6	1.36364	4	100

Inhibition by ScF_x:

- Follow same protocol as for AlF_x

ScF_x Stock	Tube #	ScF_x (µl)	[ScF_x] (µM)	T8 (µl)	Cocktail (µl)
	0	0	0	10	100
1.03 mM	1	2	0.019	8	100
	2	3	0.028	7	100
	3	4	0.037	6	100
	4	5	0.047	5	100
	5	6	0.056	4	100
	6	7	0.065	3	100
	7	8	0.075	2	100
	8	1	0.094	9	100
10.3 mM	9	1.5	0.14	8.5	100
	10	2.5	0.234	7.5	100
	11	3.5	0.33	6.5	100
	12	5	0.468	5	100
	13	5.5	0.515	4.5	100
	14	6	0.66	4	100
	15	8.5	0.796	1.5	100
	16	10	0.936	0	100

Appendix D

Raw Data

Growth Yield in Limiting Glucose for Multiple VISIT Mutants

Plasmid	Mutation	% Avg. OD
WT	N/A	100
pSN6	βY331W	94
pUC118	UNC-	37
pLEB1	αV345R/βY331W	46
pLEB2	αI346R/βY331W	74
pLEB3	αS347R/βY331W	46
pLEB4	αI348R/βY331W	64
pLEB5	αT349R/βY331W	49
pLEB6	αV345D/βY331W	75
pLEB7	αI346D/βY331W	76
pLEB8	αS347D/βY331W	46
pLEB9	αI348D/βY331W	77
pLEB10	αT349D/βY331W	61
pLEB11	αI346A/βY331W	99
pLEB12	αI348A/βY331W	92
pLEB13	αT349A/βY331W	54
pLEB14	βR182A/βY331W	46
pLEB15	αT349R/βR182A/βY331W	48

Average optical density calculated from at least two replicates.

Biochemical Assay Data

In all tables below, data averaged from duplicate assay tubes.

Inhibiton of ATPsynthase by NBD-Cl (1)						
Strain	WT	pLEB5 (αT349R/ βY331W)	pLEB10 (αT349R/ βY331W)	pLEB13 (αT349R/ βY331W)	pLEB14 (αT349R/ βY331W)	pLEB15 (αT349R/ βY331W)
Amount of Mbr (mg)	0.02	0.08	0.02	0.02	0.01	0.01
Icubation time with ATP (min)	5	90	60	10	90	90
Average OD700 at varying [NBD-Cl] (μM)						
0	0.59	0.59	0.42	0.37	0.30	0.34
5	0.46	0.52	0.39	0.31	0.31	0.33
10	0.48	0.53	0.38	0.27	0.31	0.34
15	0.41	0.56	0.34	0.27	0.31	0.33
20	0.36	0.42	0.31	0.25	0.29	0.33
25	0.30	0.38	0.30	0.21	0.29	0.32
40	0.21	0.30	0.24	0.18	0.29	0.33
50	0.18	0.30	0.22	0.16	0.27	0.34
75	0.11	0.27	0.19	0.13	0.24	0.29
100	0.09	0.22	0.17	0.11	0.23	0.27
150	0.08	0.20	0.15	0.11	0.23	0.27
200	0.07	0.26	0.15	0.11	0.25	0.27
250	0.08	0.21	0.16	0.13	0.24	0.28
300	0.07	0.21	0.14	0.11	0.24	0.31
400	0.07	0.21	0.15	0.11	0.24	0.27
Average Blank OD700	0.06	0.13	0.11	0.13	0.16	0.18

Inhibiton of ATPsynthase by NBD-Cl (2)						
Amount of Mbr (mg)		0.08	0.02	0.02	0.08	0.08
Icubation time with ATP (min)		90	60	10	90	90
Average OD700 at varying [NBD-Cl] (μM)						
0		0.65	0.43	0.37	0.33	0.38
5		0.65	0.40	0.30	0.34	0.38
10		0.61	0.35	0.27	0.33	0.41
15		0.56	0.35	0.23	0.33	0.33
20		0.48	0.31	0.21	0.30	0.36
25		0.42	0.26	0.19	0.32	0.39
40		0.40	0.23	0.15	0.32	0.33
50		0.33	0.22	0.15	0.28	0.37
75		0.28	0.17	0.12	0.27	0.29
100		0.23	0.16	0.12	0.24	0.29
150		0.22	0.15	0.11	0.26	0.29
200		0.24	0.15	0.12	0.26	0.27
250		0.25	0.15	0.12	0.25	0.26
300		0.22	0.16	0.12	0.24	0.29
400		0.22	0.15	0.10	0.25	0.26
Average Blank OD700		0.14	0.11	0.11	0.15	0.15

Inhibiton of ATPsynthase by NBD-Cl (3)						
Strain	WT	pLEB5 (αT349R/ βY331W)	pLEB10 (αT349R/ βY331W)	pLEB13 (αT349R/ βY331W)	pLEB14 (αT349R/ βY331W)	pLEB15 (αT349R/ βY331W)
Amount of Mbr (mg)					0.1	0.1
Icubation time with ATP (min)					120	120
Average OD700 at varying [NBD-Cl] (μM)						
					0.31	0.38
					0.29	0.36
					0.30	0.39
					0.29	0.39
					0.27	0.38
					0.28	0.31
					0.27	0.33
					0.25	0.35
					0.23	0.30
					0.22	0.28
					0.21	0.27
					0.22	0.27
					0.22	0.27
					0.22	0.28
					0.21	0.30
Average Blank OD700					0.15	0.16
Inhibiton of ATPsynthase by NBD-Cl (4)						
Amount of Mbr (mg)					0.1	0.1
Icubation time with ATP (min)					120	120
Average OD700 at varying [NBD-Cl] (μM)						
					0.31	0.37
					0.30	0.37
					0.27	0.36
					0.31	0.36
					0.30	0.36
					0.29	0.35
					0.27	0.33
					0.25	0.33
					0.22	0.30
					0.22	0.29
					0.21	0.27
					0.24	0.27
					0.22	0.26
					0.21	0.26
					0.21	0.26
Average Blank OD700					0.15	0.15

DTT Reversibility of ATPsynthase Inhibiton by NBD-Cl (1)							
Strain		WT	pLEB5 (αT349R/ βY331W)	pLEB10 (αT349R/ βY331W)	pLEB13 (αT349R/ βY331W)	pLEB14 (αT349R/ βY331W)	pLEB15 (αT349R/ βY331W)
Amount of Mbr (mg)		0.02	0.08	0.02	0.02	0.1	0.1
Icubation time with ATP (min)		7	90	60	20	90	90
Tube	Average OD700						
1	Mbr only	1.01	0.65	0.81	0.92	0.28	0.33
2	NBD-Cl+DTT	0.61	0.46	0.55	0.57	0.21	0.22
3	DTT	0.94	0.70	0.87	0.96	0.31	0.38
4	NBD-Cl	0.08	0.21	0.09	0.04	0.20	0.30
1	Blank 1	0.08	0.11	0.05	0.07	0.15	0.17
2	Blank 2	0.06	0.11	0.04	0.10	0.09	0.10
3	Blank 3	0.06	0.11	0.05	0.07	0.15	0.17
4	Blank 4	0.07	0.11	0.04	0.07	0.16	0.17

DTT Reversibility of ATPsynthase Inhibiton by NBD-Cl (2)							
Amount of Mbr (mg)		0.02	0.08	0.02	0.02	0.1	0.1
Icubation time with ATP (min)		7	90	60	20	90	90
Tube	Average OD700						
1	Mbr only	1.00	0.68	0.74	1.03	0.28	0.35
2	NBD-Cl+DTT	0.62	0.58	0.43	0.56	0.18	0.25
3	DTT	0.79	0.68	1.09	0.91	0.32	0.38
4	NBD-Cl	0.09	0.20	0.11	0.10	0.20	0.27
1	Blank 1	0.07	0.11	0.05	0.11	0.14	0.16
2	Blank 2	0.06	0.11	0.05	0.12	0.08	0.11
3	Blank 3	0.06	0.11	0.05	0.11	0.14	0.24
4	Blank 4	0.07	0.11	0.05	0.12	0.14	0.18

DTT Reversibility of ATPsynthase Inhibiton by NBD-Cl (3)							
Strain		WT	pLEB5 (αT349R/ βY331W)	pLEB10 (αT349R/ βY331W)	pLEB13 (αT349R/ βY331W)	pLEB14 (αT349R/ βY331W)	pLEB15 (αT349R/ βY331W)
Amount of Mbr (mg)		0.08	0.02	0.02	0.02	0.1	
Icubation time with ATP (min)		90	60	60	20	120	
Tube	Average OD700						
1	Mbr only	0.88	0.58	0.73	1.33	0.23	
2	NBD-Cl+DTT	0.64	0.52	0.61	0.97	0.27	
3	DTT	0.92	0.64	0.73	0.93	0.26	
4	NBD-Cl	0.12	0.17	0.14	0.09	0.16	
1	Blank 1	0.10	0.09	0.08	0.05	0.11	
2	Blank 2	0.10	0.09	0.08	0.06	0.15	
3	Blank 3	0.09	0.09	0.08	0.06	0.15	
4	Blank 4	0.10	0.09	0.08	0.06	0.14	

DTT Reversibility of ATPsynthase Inhibiton by NBD-Cl (4)							
Amount of Mbr (mg)		0.08	0.02	0.02	0.02	0.1	
Icubation time with ATP (min)		90	60	60	20	120	
Tube	Average OD700						
1	Mbr only	0.86	0.62	0.74	0.94	0.30	
2	NBD-Cl+DTT	0.60	0.50	0.55	0.67	0.40	
3	DTT	0.82	0.59	0.74	0.55	0.28	
4	NBD-Cl	0.11	0.18	0.13	0.08	0.23	
1	Blank 1	0.09	0.09	0.08	0.04	0.15	
2	Blank 2	0.08	0.09	0.08	0.06	0.17	
3	Blank 3	0.08	0.10	0.08	0.07	0.16	
4	Blank 4	0.09	0.12	0.08	0.07	0.17	

Inhibiton of ATPsynthase by an Extra Pulse of NBD-Cl (1)							
Strain		WT	pLEB5 (αT349R/ βY331W)	pLEB10 (αT349R/ βY331W)	pLEB13 (αT349R/ βY331W)	pLEB14 (αT349R/ βY331W)	pLEB15 (αT349R/ βY331W)
Amount of Mbr (mg)		0.02	0.08	0.02	0.02	0.1	0.1
Icubation time with ATP (min)		6	90	60	15	90	90
Tube	Average OD700						
B1	Blank 1	0.04	0.05	0.03	0.04	0.10	0.10
B2	Blank 2	0.04	0.06	0.04	0.04	0.10	0.10
B3	Blank 3	0.04	0.05	0.03	0.04	0.10	0.10
1	Mbr only	0.62	0.56	0.36	0.55	0.23	0.26
2	NBD-Cl (150 μM)	0.07	0.16	0.06	0.05	0.17	0.21
3	NBD-Cl (150 μM + 150 μM)	0.05	0.13	0.05	0.05	0.15	0.20
Inhibiton of ATPsynthase by an Extra Pulse of NBD-Cl (2)							
Amount of Mbr (mg)		0.02	0.08	0.02	0.02	0.1	0.1
Icubation time with ATP (min)		6	90	60	15	90	90
Tube	Average OD700						
B1	Blank 1	0.056	0.052	0.034	0.044	0.104	0.104
B2	Blank 2	0.056	0.059	0.033	0.040	0.100	0.110
B3	Blank 3	0.056	0.055	0.034	0.038	0.098	0.106
1	Mbr only	0.729	0.550	0.386	0.497	0.229	0.277
2	NBD-Cl (150 μM)	0.078	0.156	0.067	0.048	0.163	0.220
3	NBD-Cl (150 μM + 150 μM)	0.062	0.124	0.050	0.045	0.158	0.195

Protection from NBD-CL Inhibiton of ATPsynthase by MgADP (1)						
Strain	WT	pLEB5 (αT349R/ βY331W)	pLEB10 (αT349R/ βY331W)	pLEB13 (αT349R/ βY331W)	pLEB14 (αT349R/ βY331W)	pLEB15 (αT349R/ βY331W)
Amount of Mbr (mg)	0.02	0.08	0.02	0.02	0.01	0.01
Icubation time with ATP (min)	5	90	60	15	90	90
Average OD700 at varying [MgADP] mM						
0	0.12	0.18	0.12	0.09	0.18	0.21
0.5	0.48	0.23	0.14	0.10	0.18	0.25
0.75	0.44	0.24	0.13	0.11	0.18	0.27
1	0.43	0.27	0.13	0.11	0.20	0.31
1.5	0.46	0.26	0.14	0.11	0.20	0.30
2	0.46	0.27	0.15	0.13	0.21	0.30
2.5	0.50	0.27	0.14	0.13	0.21	0.31
3	0.50	0.29	0.16	0.14	0.22	0.31
3.5	0.50	0.30	0.16	0.15	0.21	0.33
4	0.49	0.29	0.17	0.16	0.22	0.34
4.5	0.51	0.31	0.23	0.18	0.22	0.35
5	0.51	0.32	0.19	0.21	0.23	0.34
5.5	0.57	0.34	0.21	0.24	0.23	0.34
6	0.59	0.30	0.22	0.21	0.23	0.36
8	0.44	0.33	0.24	0.26	0.24	0.35
10	0.69	0.37	0.26	0.31	0.24	0.37
12	0.83	0.40	0.30	0.36	0.26	0.36
Blank 0	0.12	0.08	0.08	0.08	0.11	0.11
Protection from NBD-CL Inhibiton of ATPsynthase by MgADP (2)						
Average OD700 at varying [MgADP] mM						
0	0.12	0.19	0.12	0.09	0.17	0.22
0.5	0.42	0.22	0.11	0.10	0.19	0.27
0.75	0.38	0.23	0.11	0.13	0.20	0.26
1	0.42	0.24	0.11	0.13	0.23	0.28
1.5	0.43	0.24	0.13	0.12	0.25	0.29
2	0.45	0.27	0.12	0.13	0.21	0.31
2.5	0.47	0.29	0.13	0.12	0.24	0.30
3	0.50	0.27	0.14	0.13	0.23	0.31
3.5	0.52	0.30	0.15	0.14	0.23	0.31
4	0.53	0.31	0.17	0.16	0.23	0.33
4.5	0.56	0.32	0.17	0.17	0.26	0.32
5	0.56	0.34	0.19	0.20	0.24	0.34
5.5	0.58	0.34	0.19	0.21	0.26	0.34
6	0.63	0.35	0.20	0.22	0.27	0.35
8	0.68	0.37	0.20	0.26	0.27	0.33
10	0.76	0.38	0.25	0.30	0.27	0.34
12	0.82	0.40	0.28	0.36	0.27	0.37
Blank 0	0.12	0.09	0.08	0.08	0.10	0.11

MgPi protection from inhibition by NBD-Cl of ATPsynthase (1)							
Strain		WT	WT Blank	pLEB5 (αT349R/ βY331W)	pLEB5 Blank	pLEB10 (αT349R/ βY331W)	pLEB10 Blank
Amount of Mbr (mg)		0.08		0.02		0.02	
Icubation time with ATP (min)		90		60		60	
Set 1 (0 mM MgPi)	Time (min)	Average OD700					
	0	0.86	0.08	0.55	0.07	0.28	0.04
	5	0.54	0.11	0.29	0.08	0.25	0.04
	10	0.37	0.09	0.22	0.07	0.18	0.04
	15	0.26	0.09	0.22	0.07	0.16	0.04
	20	0.17	0.08	0.19	0.07	0.13	0.04
	25	0.15	0.09	0.17	0.08	0.10	0.04
	30	0.13	0.08	0.15	0.07	0.11	0.04
	35	0.10	0.08	0.15	0.07	0.09	0.04
	40	0.09	0.07	0.17	0.07	0.09	0.04
	60	0.08	0.06	0.18	0.08	0.07	0.04
Set 2 (2.5 mM MgPi)	Time (min)	Average OD700					
	0	0.77	0.08	0.55	0.08	0.50	0.05
	5	0.50	0.08	0.58	0.37	0.55	0.31
	10	0.91	0.38	0.57	0.37	0.52	0.31
	15	0.95	0.38	0.55	0.38	0.49	0.31
	20	0.76	0.36	0.54	0.37	0.49	0.31
	25	0.74	0.37	0.53	0.36	0.49	0.32
	30	0.73	0.36	0.55	0.34	0.45	0.32
	35	0.70	0.36	0.52	0.36	0.48	0.32
	40	0.62	0.36	0.51	0.36	0.42	0.32
	60	0.55	0.39	0.48	0.35	0.39	0.32
Set 3 (5 mM MgPi)	Time (min)	Average OD700					
	0	0.77	0.07	0.57	0.08	0.50	0.05
	5	0.55	0.09	0.87	0.64	0.79	0.57
	10	1.22	0.64	0.87	0.64	0.76	0.57
	15	1.16	0.64	0.85	0.64	0.74	0.57
	20	1.14	0.64	0.84	0.68	0.74	0.57
	25	1.03	0.63	0.85	0.64	0.71	0.57
	30	1.05	0.62	0.84	0.64	0.72	0.57
	35	1.05	0.61	0.82	0.66	0.69	0.57
	40	0.96	0.61	0.82	0.65	0.68	0.57
	60	0.83	0.63	0.78	0.64	0.63	0.54
Set 4 (10 mM MgPi)	Time (min)	Average OD700					
	0	0.09	0.79	0.57	0.08	0.49	0.05
	5	0.10	0.56	1.36	1.16	1.24	1.06
	10	1.14	1.59	1.40	1.17	1.20	1.05
	15	1.15	1.55	1.34	1.17	1.21	1.06
	20	1.27	1.59	1.37	1.21	1.19	1.07
	25	1.18	1.49	1.37	1.22	1.18	1.06
	30	1.15	1.53	1.35	1.18	1.18	1.09
	35	1.16	1.50	1.34	1.17	1.18	1.07
	40	1.13	1.49	1.32	1.18	1.17	1.08
	60	1.14	1.33	1.32	1.16	1.12	1.06

MgPi protection from inhibition by NBD-Cl of ATPsynthase (1)							
Strain		pLEB13	pLEB13	pLEB14	pLEB14	pLEB15	pLEB15
Amount of Mbr (mg)		0.02		0.1		0.1	
Icubation time with ATP (min)		20		120		90	
Set 1 (0 mM MgPi)	Time (min)	Average OD700					
	0	0.37	0.05	0.22	0.06	0.25	0.06
	5	0.37	0.05	0.16	0.07	0.22	0.07
	10	0.23	0.05	0.15	0.06	0.20	0.07
	15	0.13	0.05	0.15	0.06	0.19	0.07
	20	0.12	0.05	0.13	0.07	0.18	0.08
	25	0.11	0.05	0.13	0.06	0.20	0.07
	30	0.08	0.05	0.14	0.06	0.18	0.07
	35	0.07	0.05	0.13	0.06	0.18	0.07
	40	0.07	0.05	0.14	0.06	0.18	0.07
	60	0.06	0.05	0.13	0.06	0.18	0.07
Set 2 (2.5 mM MgPi)	Time (min)	Average OD700					
	0	0.38	0.05	0.20	0.08	0.25	0.09
	5	0.80	0.33	0.45	0.34	0.46	0.33
	10	0.74	0.33	0.43	0.36	0.47	0.33
	15	0.66	0.33	0.42	0.36	0.47	0.33
	20	0.66	0.33	0.43	0.36	0.46	0.33
	25	0.60	0.33	0.46	0.35	0.47	0.33
	30	0.62	0.34	0.43	0.36	0.45	0.33
	35	0.57	0.33	0.42	0.37	0.46	0.34
	40	0.56	0.34	0.43	0.35	0.46	0.34
	60	0.53	0.34	0.43	0.35	0.43	0.33
Set 3 (5 mM MgPi)	Time (min)	Average OD700					
	0	0.36	0.05	0.19	0.07	0.26	0.07
	5	1.02	0.61	0.69	0.61	0.76	0.61
	10	0.98	0.60	0.69	0.62	0.77	0.62
	15	0.94	0.61	0.69	0.64	0.76	0.64
	20	0.89	0.60	0.70	0.64	0.75	0.62
	25	0.90	0.61	0.72	0.62	0.76	0.62
	30	0.87	0.59	0.70	0.62	0.74	0.63
	35	0.80	0.60	0.70	0.61	0.74	0.61
	40	0.83	0.61	0.70	0.62	0.76	0.63
	60	0.77	0.59	0.69	0.62	0.74	0.62
Set 4 (10 mM MgPi)	Time (min)	Average OD700					
	0	0.42	0.05	0.20	0.08	0.27	0.07
	5	1.45	1.11	1.20	1.11	1.25	1.12
	10	1.42	1.11	1.19	1.13	1.28	1.11
	15	1.40	1.11	1.19	1.14	1.27	1.13
	20	1.34	1.12	1.23	1.12	1.25	1.12
	25	1.38	1.11	1.19	1.13	1.24	1.15
	30	1.34	1.12	1.21	1.13	1.26	1.13
	35	1.33	1.10	1.20	1.12	1.28	1.14
	40	1.34	1.13	1.21	1.13	1.24	1.14
	60	1.30	1.13	1.19	1.12	1.23	1.14

MgPi protection from inhibition by NBD-Cl of ATPsynthase (2)					
Strain		WT	WT Blank	pLEB13 (αT349R/ βY331W)	pLEB13 Blank
Amount of Mbr (mg)		0.08		0.02	
Icubation time with ATP (min)		90		20	
	Time (min)	Average OD700			
Set 1 (0 mM MgPi)	0	0.95	0.08	0.55	0.04
	5	0.50	0.08	0.26	0.04
	10	0.36	0.07	0.19	0.05
	15	0.25	0.07	0.13	0.07
	20	0.18	0.07	0.16	0.05
	25	0.15	0.07	0.13	0.04
	30	0.11	0.07	0.08	0.04
	35	0.10	0.07	0.06	0.05
	40	0.16	0.06	0.06	0.07
	60	0.08	0.05	0.05	0.05
	Time (min)	Average OD700			
Set 2 (2.5 mM MgPi)	0	0.91	0.09	0.53	0.06
	5	0.99	0.35	0.61	0.31
	10	0.96	0.35	0.63	0.31
	15	0.88	0.34	0.62	0.34
	20	0.79	0.35	0.56	0.31
	25	0.82	0.34	0.50	0.34
	30	0.78	0.34	0.52	0.31
	35	0.78	0.34	0.50	0.32
	40	0.72	0.35	0.54	0.32
	60	0.56	0.33	0.53	0.32
	Time (min)	Average OD700			
Set 3 (5 mM MgPi)	0	0.92	0.09	0.52	0.05
	5	1.17	0.60	0.87	0.59
	10	1.17	0.60	0.86	0.56
	15	1.09	0.60	0.83	0.57
	20	1.10	0.61	0.79	0.57
	25	1.10	0.60	0.78	0.56
	30	1.02	0.60	0.78	0.57
	35	1.01	0.61	0.75	0.58
	40	0.96	0.61	0.75	0.58
	60	0.84	0.59	0.70	0.57
	Time (min)	Average OD700			
Set 4 (10 mM MgPi)	0	0.91	0.11	0.56	0.07
	5	1.56	1.12	1.33	1.04
	10	1.54	1.13	1.28	1.05
	15	1.51	1.12	1.30	1.04
	20	1.53	1.12	1.28	1.08
	25	1.50	1.12	1.26	1.07
	30	1.46	1.11	1.26	1.08
	35	1.51	1.11	1.29	1.06
	40	1.43	1.11	1.22	1.07
	60	1.36	1.12	1.23	1.09

Appendix E

Mutagenic Oligonucleotides

Mutant	Mutation Site	Forward Primer	Original codon→ Mutant codon	Enzyme
pLEB1	αV345R/βY331W	GCGTTCGTTCCGACCAAC**CGA**ATTTC CATTACCGATGGTCAG	GTA→CGA ATC→ATT (SM)	ApoI
pLEB2	αI346R/βY331W	CGTTCGTTCCGACCAACGTA**AGA**TCT ATTACCGATGGTCAGATCTTC	ATC→AGA TCC→TCT (SM)	BglII
pLEB3	αS347R/βY331W	TTCGTTCCGACCAACGTAATC**CGG**AT TACCGATGGTCAGATCTTC	TCC→CGG	BspEI
pLEB4	αI348R/βY331W	CGTTCGTTCCGACCAACGTAATCTCT**A GA**ACCGATGGTCAGATCTTCCTG	ATT→AGA TCC→TCT (SM)	XbaI
pLEB5	αT349R/βY331W	GTTCCGACCAACGTAATCTCCATT**CG C**GATGGTCAGATCT	ACC→CGC	NruI
pLEB6	αV345D/βY331W	CGTTCGTTCCGACCAAC**GAT**ATCTCC ATTACCGATGGT	GTA→GAT	EcoRV
pLEB7	αI346D/βY331W	CGTTCGTTCCGACCAACGTA**GAC**TCC ATTACCGATGG	ATC→GAC	AccI
pLEB8	αS347D/βY331W	GTTCGTTCCGACCAACGTAATC**GAT**A TCACCGATGGTCAGATCTTCCTGG	TCC→GAT ATT→ATC (SM)	EcoRV
pLEB9	αI348D/βY331W	CGTTCCGACCAACGTAATCTC**AGAT**A CCGATGGTCAGATCTTCCT	ATT→GAT TCC→TCA (SM)	DdeI
pLEB10	αT349D/βY331W	GTTCCGACCAACGTAATCTCAATT**GA C**GATGGTCAGATCTTCCTGG	ACC→GAC TCC→TCA (SM)	MfeI
pLEB11	αI346A/βY331W	TTCTGCGTTCGTTCCGACCAACGTG**GC G**TCCATAACCGATGGTCAG	ATC→GCG GTA→GTG (SM)	BsaHI
pLEB12	αI348A/βY331W	GTTCGTTCCGACCAACGTAATCAGC**G CT**ACCGATGGTCAGATCTTCC	ATT→GCT TCC→AGC (SM)	HaeII
pLEB13	αT349A/βY331W	GTTCCGACCAACGTAATCTATA**GCC**G ATGGTCAGATCTTCCTG	ACC→GCC TCC→TCT(SM) ATT→ATA (SM)	SfcI
pLEB14	βR182A/βY331W	GTTTGCGGGCGTAGGTGAA**GCT**ACTC GTGAGG	CGT→GCT	AluI
pLEB15	αT349R/βR182A/ βY331W	Primer for pLEB14 used on pLEB5 plasmid.	See pLEB14 and pLEB5	AluI NruI

Name of the constructed plasmid is shown next to the mutation. βY331W was used in all newly constructed plasmids. Forward primers are shown with underlined nucleotides denoting the newly inserted mutation. Silent mutations (SM) were introduced in some plasmids. New restriction sites were inserted into all mutants; however, restriction analysis was not performed before or after sequencing.

VITA

LAURA E. BRUDECKI

Personal Data:	Date of Birth: January 29, 1986 Place of Birth: Morristown, TN Marital Status: Single
Education:	B.S. Biology; Biochemistry Concentration East Tennessee State University, Johnson City, Tennessee 2008 M.S. Biology East Tennessee State University, Johnson City, Tennessee 2010
Professional Experience:	Graduate Assistant, ETSU 2009-2010 Instructor, Biology 1121 for Science Majors, ETSU Spring 2009-Spring 2010 Instructor, Biology 1011 for Non-Science Majors, ETSU Summer 2010 Fall 2010
Publications:	Brudecki, L. E., Grindstaff, J. J., and Ahmad, Z. (2008) Role of αPhe-291 Residue in the Phosphate-Binding Subdomain of Catalytic Sites of *Escherichia coli* ATP Synthase. *Archives of Biochemistry and Biophysics* **471,** 168-175. Li, W., Brudecki, L. E., Senior, A. E., and Ahmad, Z. (2009) Role of α-Subunit VISIT-DG Sequence Residues Ser-347 and Gly-351 in the Catalytic Sites of *Escherichia coli* ATP Synthase. *Journal of Biological Chemistry* **284,** 10747-10754. Ahmad, Z., and Brudecki, L. E. (2010) Molecular Modulation of the Alpha-Subunit VISIT-DG Sequence in the Catalytic Sites of *Escherichia coli* ATP synthase. *FASEB Journal* **24,** 463.1
Honors and Awards:	ETSU James H. Quillen Scholar 2009-2010 ETSU Student-Faculty Collaborative Research Grant 2008